https://doi.org/10.5194/egusphere-2024-1315
Preprint. Discussion started: 14 May 2024

Methane, carbon dioxide and nitrous oxide emissions from two clear-water and two turbid-water urban ponds in Brussels (Belgium)

Thomas Bauduin [1,2], Nathalie Gypens [1], Alberto V. Borges [2]

[1]Ecology of Aquatic Systems, Université Libre de Bruxelles, Belgium
[2]Chemical Oceanography Unit, University of Liège, Belgium

Correspondence to: Thomas Bauduin (thomas.bauduin@ulb.be)

Abstract. Shallow ponds can exist in a clear-water state dominated by macrophytes or a turbid-water state dominated by phytoplankton, but it is unclear if these two states affect differently carbon dioxide (CO_2), methane (CH_4) and nitrous oxide (N_2O) emissions to the atmosphere. Two clear-water urban ponds (Silex and Tenreuken) dominated by macrophytes, and two turbid-water urban ponds (Leybeek and Pêcheries) dominated by phytoplankton, in the city of Brussels (Belgium), were sampled 46 times between June 2021 and December 2023 to measure the partial pressure of CO_2 (pCO_2), dissolved CH_4 concentration, N_2O saturation level ($\%N_2O$), and ancillary variables. CH_4 ebullitive fluxes were also measured in the four ponds during 8 deployments, totally 48 days of cumulated measurements. The $^{13}C/^{12}C$ ratio of CH_4 ($\delta^{13}C$-CH_4) was measured in bubbles from the sediment and in water to decipher the pathway of sedimentary methanogenesis (acetoclastic or hydrogenotrophic) and quantify methane oxidation (MOX) in the water column. The pCO_2 and CH_4 values in the sampled urban ponds correlated with precipitation and water temperature, respectively. The $\%N_2O$ values did not correlate with dissolved inorganic nitrogen (DIN) nor other variables for the individual ponds, but a positive relation to DIN emerged from the combined data-set for the four ponds. The sampled turbid-water and clear-water ponds did not show differences in terms of diffuse emissions of CO_2 and N_2O. Clear-water ponds exhibited higher values of annual ebullitive CH_4 fluxes compared to turbid-water ponds, most probably in relation to the delivery to sediments of organic matter from macrophytes. At seasonal scale, CH_4 fluxes between the surface of the ponds and the atmosphere exhibited a temperature dependence in all four ponds, with ebullitive CH_4 fluxes having a stronger dependence to temperature than diffusive CH_4 fluxes. The temperature sensitivity of ebullitive CH_4 fluxes was different among the four ponds and decreased with increasing water depth. During summer 2023, hydrogenotrophic methanogenesis pathway seemed to dominate in clear-water ponds and acetoclastic methanogenesis pathway seemed to dominate in turbid-water ponds, as indicated by the $\delta^{13}C$-CH_4 values of bubbles sampled by physically perturbing sediments. The $\delta^{13}C$-CH_4 values of bubbles sampled during bubble trap deployments in 2021-2023 indicated a seasonal shift to hydrogenotrophic methanogenesis pathway in fall compared to spring and summer, when acetoclastic methanogenesis pathway seemed to dominate. The $\delta^{13}C$-CH_4 of dissolved CH_4 indicated higher rates of MOX in turbid-water ponds compared to clear-water ponds, with an overall positive correlation with total suspended matter (TSM) and Chlorophyll-*a* (Chl-*a*) concentrations. The presence of suspended particles putatively enhanced MOX by reducing light inhibition of MOX and/or by serving as substrate for fixed methanotrophic bacteria in the water column. Total CH_4 emissions in CO_2 equivalents either equalized or exceeded those of CO_2 in most ponds, while N_2O emissions were negligible compared to the other two greenhouse gases (GHGs). Total annual GHG emissions in CO_2 equivalents from all four ponds increased from 2022 to 2023 due to higher CO_2 diffusive fluxes, likely driven by higher annual precipitation in 2023 compared to 2022, possibly in response to the intense El Niño event of 2023.

https://doi.org/10.5194/egusphere-2024-1315
Preprint. Discussion started: 14 May 2024

1. Introduction

Emissions to the atmosphere from inland waters (rivers, lakes, and reservoirs) of greenhouse gases (GHGs) such as carbon dioxide (CO_2), methane (CH_4) and nitrous oxide (N_2O) are quantitatively important for global budgets (Lauerwald et al., 2023). Emissions from lakes are lower than from rivers for CO_2 (Raymond et al., 2013) and N_2O (Lauerwald et al., 2019; Maavara et al., 2019). However, emissions of CH_4 from lakes (Rosentreter et al., 2021; Johnson et al., 2022) are significant compared to rivers (Stanley et al., 2016; Rocher-Ros et al., 2023). The contribution of CO_2 and CH_4 emissions from small water bodies (ponds) could be disproportionately high compared to large systems (Holgerson and Raymond, 2016) as shallow lakes are the most abundant of all lake types in number (Verpoorter et al., 2014, Cael et al., 2017). The emissions of GHGs from artificial ponds (agricultural reservoirs, urban ponds, storm-water retention basins, …) could be higher than those from natural systems (Martinez-Cruz et al., 2017; Grinham et al., 2018; Herrero Ortega et al., 2019; Gorsky et al., 2019; Ollivier et al., 2019; Peacock et al., 2019, 2021; Webb et al., 2019; Bauduin et al., 2024). This seems to result from higher external inputs of anthropogenic carbon and nitrogen in artificial systems but might also reflect other differences compared to natural systems such as in hydrology (Clifford and Heffernan, 2018). Among artificial systems, urban ponds have been seldom investigated for GHG emissions (Singh et al., 2000; Natchimuthu et al., 2014; van Bergen et al., 2019; Audet et al., 2020; Peacock et al., 2021; Bauduin et al., 2024). Urban areas have many small artificial water bodies mostly associated to green spaces such as public parks, and their number is increasing due to rapid urbanisation worldwide (Brans et al., 2018; Audet et al., 2020). Urban ponds are generally small, shallow, and surrounded by impervious surfaces (Davidson et al., 2015; Peacock et al., 2021). Runoff results in high inputs of organic matter and dissolved inorganic nitrogen (DIN) that sustain production and emission of CO_2, CH_4, and N_2O to the atmosphere.

In shallow ponds and lakes, including urban ponds, submerged aquatic primary production is either dominated by submerged macrophytes or by phytoplankton, corresponding to two alternate states (Scheffer et al., 1993). These two alternative states correspond to clear waters or turbid waters, during the productive periods of year (summer in mid-latitudes). The presence of macrophytes strongly affects CH_4 cycling in freshwaters (Bastviken et al., 2023) and vegetated littoral zones of lakes exhibit higher CH_4 emissions than non-vegetated (Desrosiers et al., 2022; Theus et al., 2023). Macrophytes influence sediment and organic matter decomposition processes depending on the quality and quantity of plant matter they release into their environment (Reitsema et al., 2018; Harpenslager et al., 2022; Theus et al., 2023). Yet, few studies have consistently compared CH_4 emissions in clear-water and turbid-water ponds (Hilt et al., 2017). A study in Argentina reported higher dissolved CH_4 concentrations in natural clear-water ponds with submerged macrophytes compared to turbid-water phytoplankton dominated ponds, but no differences in measured CH_4 emissions (Baliña et al., 2023). The presence of macrophytes also strongly influences nitrogen cycling in sediments of lakes and ponds (Barko et al., 1991; Choudhury et al., 2018; Deng et al., 2020; Dan et al., 2021) and should in theory also affect N_2O emissions, although seldom investigated, and available studies provide contradictory conclusions. Ni et al. (2022) showed that N_2O emissions followed diurnal cycles, peaking in the middle of the day when O_2 concentrations were maximal in areas dominated by submerged macrophytes in Lake Wuliangsuhai (China). Yang et al. (2012) showed that N_2O emissions followed the seasonal cycle of aboveground biomass of emerged macrophytes (*Phragmites*) in Baiyangdian Lake (China). On the contrary, some studies showed there were no significant differences of denitrification and N_2O production in sediments of macrophyte-rich (n=10) and macrophyte-free (n=12) lakes in subtropical China (Liu et al., 2018).

The emissions from aquatic systems of CO_2 and N_2O are exclusively through diffusion across the air-water interface (diffusive flux), while CH_4 can be additionally emitted as bubbles released from sediments to the atmosphere (ebullitive flux). The ebullitive CH_4 flux usually represents more than half of total (diffusive+ebullitive) CH_4 emissions from shallow lakes (Wik et

https://doi.org/10.5194/egusphere-2024-1315
Preprint. Discussion started: 14 May 2024

al., 2013; Deemer and Holgerson, 2021). Ebullitive CH_4 fluxes are particularly high in the littoral zone of lakes at depths <5 m (Wik et al., 2013; DelSontro et al., 2016; Borges et al., 2022) and strongly increase in response to temperature (DelSontro et al., 2016; Aben et al., 2017), as well as organic matter availability (DelSontro et al., 2016; 2018). Ebullitive CH_4 fluxes tend to be higher in small and shallow water bodies (Deemer and Holgerson, 2021) but are notoriously variable in time and are difficult to estimate reliably (DelSontro et al., 2011).

Here, we report a dataset of CO_2, CH_4, and N_2O dynamics in four shallow and small urban ponds (Leybeek, Pêcheries, Silex, and Tenreuken) in the city of Brussels (Belgium) (Fig. 1). Data were collected 46 times on each pond between June 2021 and December 2023 at a frequency ranging from one (winter) to three (summer) times per month at a single fixed station in each of the four ponds. The air-water diffusive fluxes of CO_2, CH_4, and N_2O were calculated from dissolved concentrations and the gas transfer velocity and the ebullitive CH_4 fluxes were measured with inverted funnels during 8 deployments (totalling 48 days) in the four ponds. The $^{13}C/^{12}C$ ratio of CH_4 ($\delta^{13}C$-CH_4) in the sedimentary bubbles and in the water provides additional information on CH_4 dynamics such as the methanogenesis pathway (acetoclastic or hydrogenotrophic) and methane oxidation (MOX).

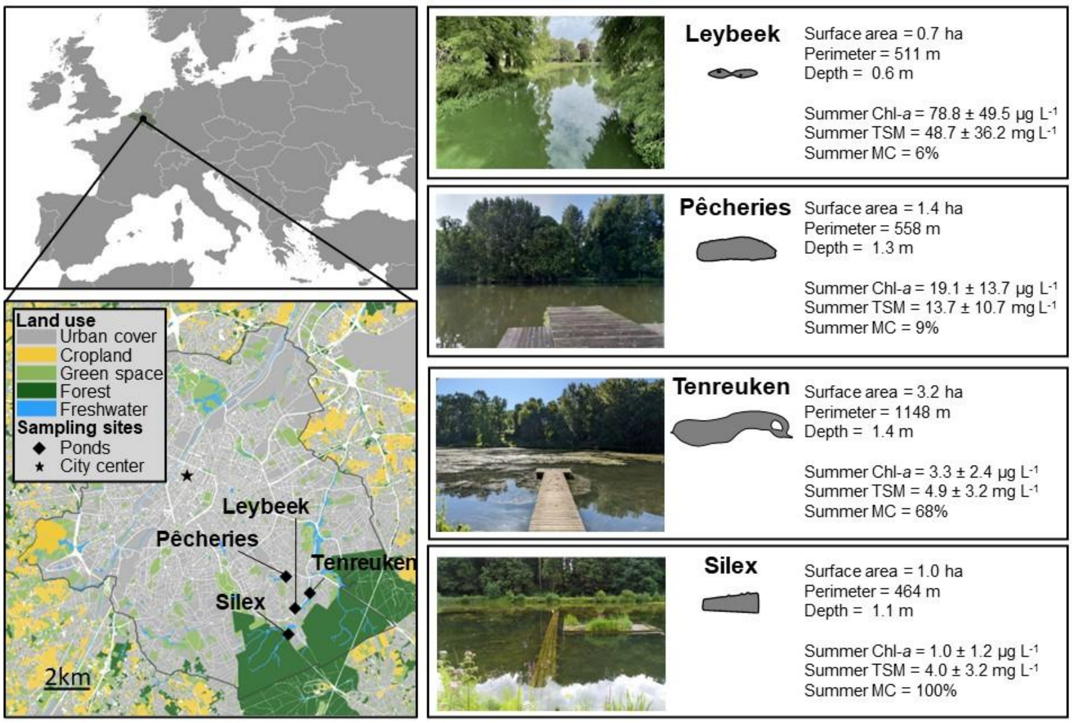

Figure 1: Location of the four sampled ponds in Brussels (Belgium, Europe). Bottom left map shows the metropolitan area of the region of Brussels delineated by the black line and surrounding region of Flanders in Belgium, showing land cover and sampled urban ponds (black diamonds). The star corresponds to the center of the city (50.8504°N, 4.3487°E). Additional information for each pond is indicated on right panels: shapes of the ponds, surface area (ha), perimeter (m), average depth (m), mean±standard deviation of summer chlorophyll-*a* (Chl-*a*, in µg L^{-1}) and summer total suspended matter (TSM, in mg L^{-1}) of periods from 21 June 21 to September 21 in 2021, 2022, 2023, and summer total macrophyte cover (MC, in %) (Table S1).

https://doi.org/10.5194/egusphere-2024-1315
Preprint. Discussion started: 14 May 2024

2. Material and Methods

2.1. Field sampling and meteorological data

Sampling was done from a pontoon, with 60ml polypropylene syringes for gases (CO_2, CH_4, N_2O) and a 2L polyethylene water container for processing at the home laboratory for other variables. Water temperature, specific conductivity, and $\%O_2$ were measured in-situ with VWR MU 6100H probe. pCO_2 was measured with a Li-Cor Li-840 infrared gas analyser (IRGA) based on the headspace technique with 4 polypropylene syringes (Borges et al., 2019). The Li-Cor 840 IRGA was calibrated before and after each cruise with ultrapure N_2 and a suite of gas standards (Air Liquide Belgium) with CO_2 mixing ratios of 388, 813, 3788 and 8300 ppm. The overall precision of pCO_2 measurements was ±2.0%. Samples for CH_4 and N_2O were transferred from the syringes with a silicone tube in 60 ml borosilicate serum bottles (Weathon), poisoned with 200 µl of a saturated solution of $HgCl_2$ and sealed with a butyl stopper and crimped with aluminium cap, without a headspace.

Surveys to identify and quantify visually the relative coverage of emerged and submerged macrophytes were conducted in summer 2023 (Table S1). This list of species of macrophytes agreed with past studies in Brussels ponds (Peretyatko et al., 2009).

Three bubble traps were deployed at 50 cm apart for measuring ebullitive CH_4 flux. The bubble traps consistent in inverted polypropylene funnels (diameter 23.5cm) mounted with 60ml polypropylene syringes and attached with steel rods to a polystyrene float. The volume of gas collected in the funnels was measured every 24 hours with 60ml syringes. The collected gas was stored in pre-evacuated 12 ml vials (Exetainers, Labco, UK) for the analysis of CH_4 concentration and $\delta^{13}C$-CH_4. The measurement series were lengthier at the Silex pond than the other three ponds, because the Silex pond is closed to the public during the week, while the other three ponds are open to the public all the time.

In summer 2023, the bubbles present in the sediment were directly sampled with bubble traps by physically perturbing the sediment with a wooden rod. These samples are referred hereafter to as from "perturbed sediments." The samples collected in the bubble traps during the ebullition measurements are referred to as from "trapped bubbles."

Air temperature, precipitation, wind speed, and atmospheric pressure, were retrieved from https://wow.meteo.be/en for the meteorological station of the Royal Meteorological Institute of St-Lambert (50.8408°N, 4.4234°E) in Brussels, located between 2.5 and 5 kilometers from the surveyed ponds. Air temperature, wind speed and atmospheric pressure were averaged over 24 h to obtain a daily mean value. Precipitation was integrated each day to obtain daily rainfall.

2.2. Laboratory analysis

2.2.1. CH_4 and N_2O measurements by gas chromatography and $\delta^{13}C$-CH_4 by cavity ring-down spectrometry

Measurements of N_2O and CH_4 concentrations dissolved in water and in the gas samples from bubbles were made with the headspace technique (20ml of ultra-pure N_2, Air Liquid Belgium, Weiss, 1981) and a gas chromatograph (GC) (SRI 8610C) with a flame ionisation detector for CH_4 (with a methanizer for CO_2) and electron capture detector for N_2O calibrated with CO_2:CH_4:N_2O:N_2 gas mixtures (Air Liquide Belgium) with mixing ratios of 1, 10 and 30 ppm for CH_4, 404, 1018, 3961 ppm for CO_2, and 0.2, 2.0 and 6.0 ppm for N_2O. The precision of measurement based on duplicate samples was ±3.9% for CH_4 and ±3.2% for N_2O.

The CO_2 concentration is expressed as partial pressure in parts per million (ppm) and CH_4 as dissolved concentration (nmol L^{-1}), in accordance with convention in existing topical literature, and because both quantities were systematically and distinctly

https://doi.org/10.5194/egusphere-2024-1315
Preprint. Discussion started: 14 May 2024

above saturation level (400 ppm and 2-3 nmol L^{-1}, respectively). Variations of N_2O were modest and concentrations fluctuated around atmospheric equilibrium, so data are presented as percent of saturation level (%N_2O, where atmospheric equilibrium corresponds to 100%).

The $\delta^{13}C$-CH_4 was measured in gas of the headspace (20ml of synthetic air, Air Liquid Belgium) equilibrated with the water sample (total volume 60ml) for water samples and directly on gas stored in Exetainers for gas samples from the bubble traps. The gas samples were diluted to obtain a final partial pressure of CH_4 in the cavity below 10 ppm to fall within the recommended operational concentration range of the instrument, prior to injection into a cavity ring-down spectrometer (G2201-I, Isotopic Analyzer, Picarro) with a Small Sample Introduction Module 2 (SSIM, Picarro). Data were corrected with curves of $\delta^{13}C$-CH_4 as a function of concentration based on two gas standards from Airgas Specialty Gases with certified $\delta^{13}C$-CH_4 values of -23.9±0.3 ‰ and -69.0±0.3 ‰.

2.2.2. Chlorophyll-a, total suspended matter, and dissolved inorganic nutrients.

Water was filtered through Whatman GF/F glass microfiber filters (porosity 0.7 µm) with a diameter of 47 mm for total suspended matter (TSM) and Chlorophyll-*a* (Chl-*a*). Filters for TSM were dried in the oven at 50C° and filters for Chl-*a* were kept frozen (-20°C). The weight of each filter was determined before and after filtration of a known volume of water using an Explorer™ Pro EP214C analytical microbalance (accuracy: ±0.1mg) for determination of TSM. Filtered water was stored in 50 ml plastic bottles and frozen (-20°C) for analysis of dissolved nutrients. Chl-*a* was measured on extracts with 90% acetone by fluorimetry (Kontron model SFM 25) (Yentsch and Menzel, 1963) with a limit of detection of 0.01 µg L^{-1}. Ammonium (NH_4^+) was determined by the nitroprusside-hypochlorite-phenol staining method (Grasshoff and Johannsen, 1972), with a limit of detection of 0.05 µmol L^{-1}. Nitrite (NO_2^-) and nitrate (NO_3^-) were determined before and after reduction of NO_3^- to NO_2^- by a cadmium-copper column, using the Griess acid reagent staining method (Grasshoff and Kremling, 2009), with a detection limit of 0.01 and 0.1 µmol L^{-1}, respectively. Soluble reactive phosphorus (SRP) was determined by the ammonium molybdate, ascorbic acid and potassium antimony tartrate staining method (Koroleff, 1983), with a limit of detection of 0.1 µmol L^{-1}. Concentration of dissolved inorganic nitrogen (DIN) was calculated as the sum NH_4^+, NO_2^- and NO_3^- concentrations.

2.3. Calculations

2.3.1. Diffusive GHG emissions

The diffusive air-water CO_2, CH_4, or N_2O fluxes (F_G) were computed according to Eq. (1):

$$F_G = k\Delta[G] \, , \tag{1}$$

where k is the gas transfer velocity and Δ[G] is the air-water gas concentration gradient. The atmospheric pCO_2 was measured on the field with the Li-Cor Li-840. A constant atmospheric concentration of 1.9 ppm was used for CH_4. The equilibrium with atmosphere for N_2O was calculated from the average air mixing ratios of N_2O provided by the Global Monitoring Division (GMD) of the National Oceanic and Atmospheric Administration (NOAA) Earth System Research Laboratory (ESRL) (Dutton et al., 2017).

k was computed from a value normalized to a Schmidt number of 600 (k_{600}) and from the Schmidt number of CO_2, CH_4 and N_2O in freshwater according to the algorithm as function of water temperature given by Wanninkhof (1992).

k_{600} was calculated from the parameterization as a function of wind speed of Cole and Caraco (1998).

https://doi.org/10.5194/egusphere-2024-1315
Preprint. Discussion started: 14 May 2024

CH_4 and N_2O emissions were converted into CO_2 equivalents (CO_2-eq) considering a 100-year timeframe, using global warming potential (GWP) of 32 and 298 for CH_4 and N_2O, respectively (Myrhe et al., 2013).

2.3.2. Ebullitive flux

Bubble flux (ml m^{-2} d^{-1}) measured with the inverted funnels was calculated according to Eq. (2):

$$F_{bubble} = \frac{V_g}{A \times \Delta t}\,, \tag{2}$$

where V_g is the volume of gas collected in the funnels (ml), A is the cross-sectional area of the funnel (m^2), Δt is the collection time (d).

A multiple linear model of F_{bubble} dependent on water temperature and drops of atmospheric pressure (Δp) was fitted to the data according to Eq. (3):

$$\log_{10}(F_{bubble}) = \alpha \times T_w + \beta \times \Delta p\,, \tag{3}$$

where α and β are the slope coefficients of the multiple linear regression model, and Δp quantifies the drops in atmospheric pressure, calculated according to Zhao et al. (2017) in Eq. (4):

$$\Delta p = -\frac{1}{\Delta t}\int_0^t p - p_0 \quad ; \quad \forall\ p < p_0\,, \tag{4}$$

where p is the atmospheric pressure, p_0 a threshold pressure fixed at 1atm and Δt the time interval between two measurements (Fig. S1).

Ebullitive CH_4 fluxes (mmol m^{-2} d^{-1}) were calculated according to Eq. (5):

$$E_{CH4} = [CH4] \times F_{bubble}\,, \tag{5}$$

where $[CH_4]$ is the CH_4 concentration in bubbles (mmol ml^{-1}).

The methane ebullition Q_{10} represents the proportional change in the ebullitive CH_4 flux per 10°C alteration in water temperature (DelSontro et al., 2016) and was computed according to Eq. (6):

$$Q_{10} = 10^{10b}\,, \tag{6}$$

where b is the slope of the linear regression between the logarithm of the ebullitive CH_4 flux (E_{CH4}) and the water temperature (T_w) and c is the y-intercept, according to Eq. (7):

$$\log_{10}(E_{CH4}) = b \times T_w + c\,, \tag{7}$$

The flux of CH_4 from dissolution of rising bubbles was computed using the model of McGinnis et al. (2006) implemented in the SiBu-GUI graphical user interface (Greinert and McGinnis, 2009).

2.3.3. Methane oxidation

The fraction of CH_4 removed (FOX) was calculated with a closed-system Rayleigh fractionation model (Liptay et al., 1998) according to Eq. (8):

https://doi.org/10.5194/egusphere-2024-1315
Preprint. Discussion started: 14 May 2024

$$\ln(1 - \mathrm{FOX}) = \frac{\ln(\delta^{13}C\text{-}CH_{4\_\mathrm{initial}}+1000) - \ln(\delta^{13}C\text{-}CH_4 + 1000)}{\alpha - 1}, \quad (8)$$

where $\delta^{13}C\text{-}CH_{4\_\mathrm{initial}}$ is the signature of dissolved CH_4 as produced by methanogenesis in sediments, $\delta^{13}C\text{-}CH_4$ is the signature of dissolved CH_4 in-situ, and α is the fractionation factor.

We used a value of 1.02 for α based on laboratory culture experiments carried out at 26°C (Coleman et al., 1981) and field measurements in three Swedish lakes (Bastviken et al., 2002) and one tropical lake (Morana et al., 2015). The α values gathered in the three Swedish lakes were independent of season and temperature according to Bastviken et al. (2002) and were very similar to those derived in a tropical lake by Morana et al. (2015).

For $\delta^{13}C\text{-}CH_{4\_\mathrm{initial}}$, we used a value of -69‰ for spring and summer, and -83‰ for fall based on average of measured $\delta^{13}C\text{-}CH_4$ in trapped bubbles (see Sect. 3.5). For winter we used a value of -76‰ corresponding to the average of the fall and spring/summer values.

MOX was indirectly determined from *FOX* and the F_G of CH_4 (F_{CH4}) according to (Bastviken et al., 2002) in Eq. (9):

$$\mathrm{MOX} = F_{CH_4} \times \frac{\mathrm{FOX}}{1 - \mathrm{FOX}}, \quad (9)$$

2.4. Statistical analysis

Statistical analysis and graphs production were conducted utilizing GraphPad Prism v10. Prior to analysis, data underwent log-transformation to ensure normality, with Shapiro tests conducted to assess distribution normality. Ordinary one-way ANOVA and Pearson's rank correlation were employed to examine differences and correlations among variables. The regressions depicted in the graphs are characterized as linear, exponential, or quadratic, and are explicitly identified when utilized.

3. Results and discussion

3.1. Seasonal variations of meteorological conditions and GHG concentrations

During the sampling period, from June 2021 to December 2023, water temperature in the surface of the four sampled ponds (Leybeek, Pêcheries, Silex, and Tenreuken; Fig. 1) tracked closely the air temperature that ranged between -1.5 and 30°C following the typical seasonal cycle at mid-latitudes in the Northern Hemisphere (Fig. S2). Years 2022 and 2023 were about 1°C warmer than the average for the period 1991-2020, while year 2021 was closer to the long-term average (Fig. 2). Year 2022 was warmer and drier than 2021 and 2023 (Fig. 2), with positive temperature anomalies observed evenly throughout the year (9 months out of 12) and negative precipitation anomalies in summer, fall and early winter (Fig. S2). Conversely, year 2021 showed warmer and drier months in June and September, colder and wetter months in July and August, and was overall wetter et colder than 2022 (Fig. 2). Year 2023 was marked by both positive temperature and precipitation anomalies (Fig. S2), resulting in a wetter and warmer year than normal compared to 2021 and 2022. (Fig. 2). Daily wind speed was generally low (<1 m s^{-1}) except for a windier period in spring 2022 (up to 5.8m s^{-1}) and in fall 2023 (up to 9.7 m s^{-1}).

https://doi.org/10.5194/egusphere-2024-1315
Preprint. Discussion started: 14 May 2024

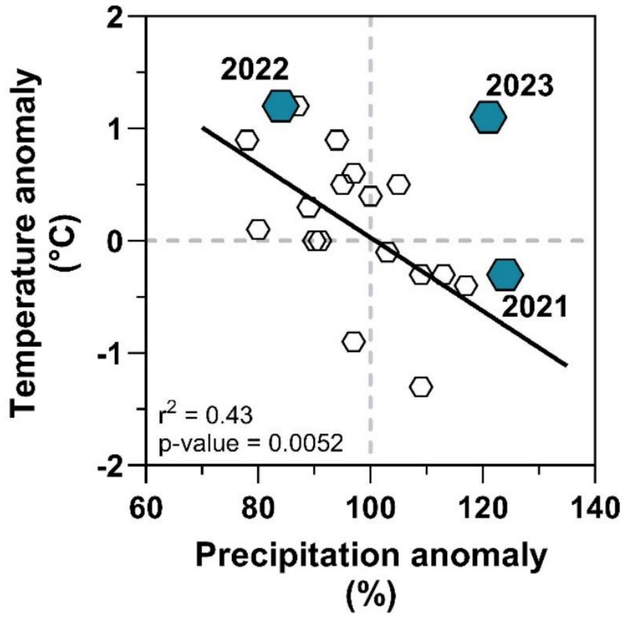

Figure 2: Temperature anomaly (difference between the average annual temperature and the normal annual temperature for the reference period, in °C) plotted against precipitation anomaly (ratio between annual precipitation and normal annual precipitation for the reference period, in %) from 2003 to 2023 for the reference period 1991-2020 in the city of Brussels (11°C and 837mm). Each hexagon represents values for years from 2003 to 2023 and filled hexagons are sampling years from this study (2021, 2022 and 2023). Linear regression for years 2003-2020 shown as black solid line (Table S5). Note the anomalous rainy year in 2023 relative to the pattern as function of temperature for the other years, possibly in response to the strong El Niño event of 2023 (Chen et al., 2024).

The four sampled ponds were in the periphery of the city of Brussels, with Silex pond bordered by the Sonian Forest (Fig. 1). The four ponds are relatively small (0.7-3.2 ha) and shallow (0.6-1.4 m) and have not been drained or dredged since at least 2018 (Table S2). The Leybeek and Pêcheries ponds had turbid-water with high summer Chl-*a* (78.8±49.5 and 19.1±13.7 µg L^{-1}, respectively) and high summer TSM (48.7±36.2 and 13.7±10.7 mg L^{-1}, respectively) concentration values, and undetectable submerged macrophyte cover in summer (Fig. 1, Table S1). Values of Chl-*a* and TSM concentrations were generally higher in the Leybeek pond compared to Pêcheries pond (Fig. 3). The Tenreuken and Silex ponds had clear-waters with low summer Chl-*a* (3.3±2.4 and 1.0±1.2 µg L^{-1}, respectively) and TSM (4.9±3.2 and 4.0±3.2 mg L^{-1}, respectively) concentration values, and a high total macrophyte cover during summer (68 and 100%, respectively). The low summer-time values of Chl-*a* and TSM concentrations in the Silex and Tenreuken ponds are probably related to competition for inorganic nutrients from macrophytes, with Silex pond showing lower Chl-*a*, lower TSM concentrations and higher summer total macrophyte cover compared to Tenreuken pond (Fig. 1).

https://doi.org/10.5194/egusphere-2024-1315
Preprint. Discussion started: 14 May 2024

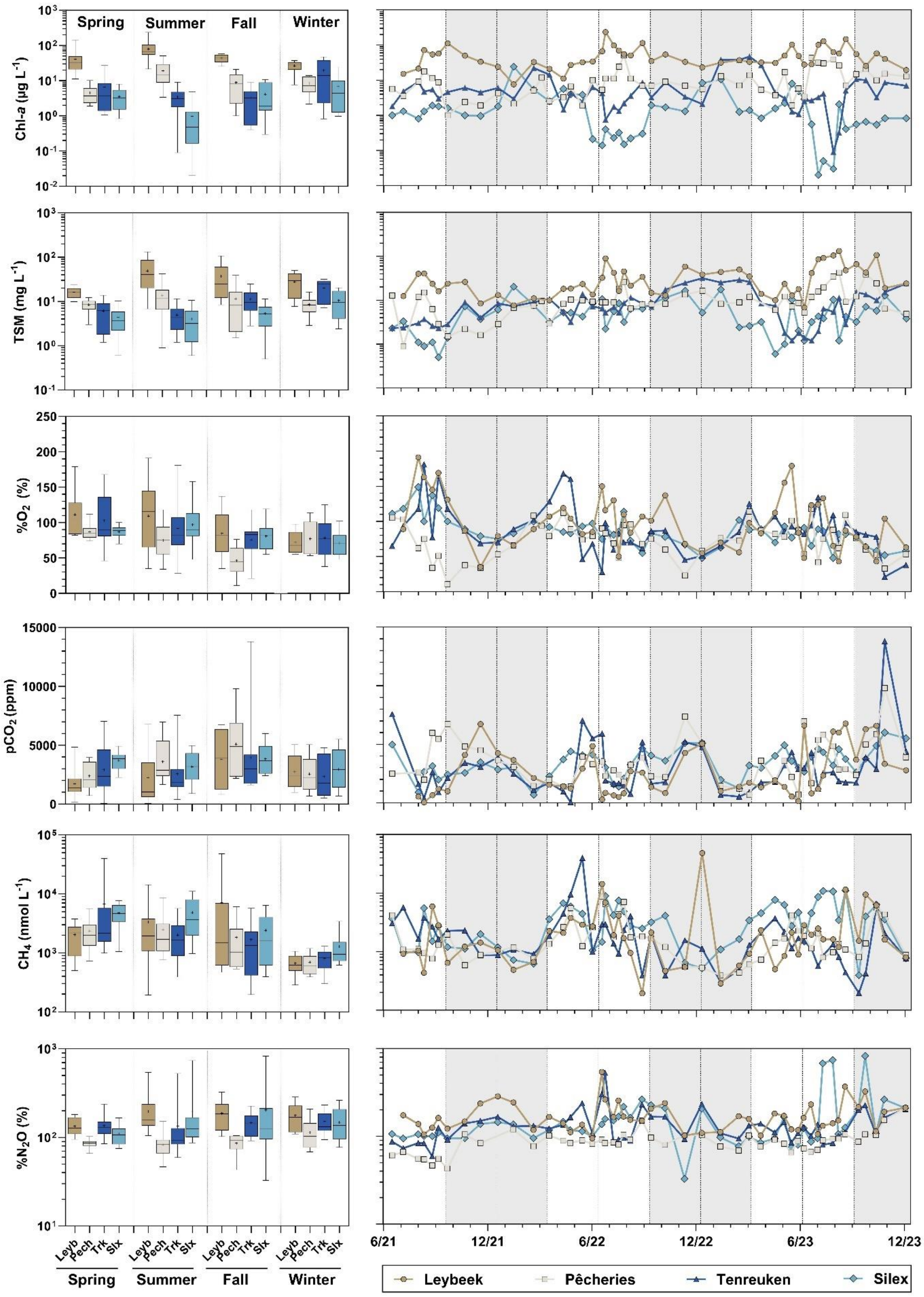

Figure 3: Seasonal variations of Chlorophyll-*a* (Chl-*a*, in µg L^{-1}); total suspended matter (TSM, in mg L^{-1}); oxygen saturation (%O_2, in %); partial pressure of CO_2 (pCO_2 in ppm); dissolved CH_4 concentration (CH_4 in nmol L^{-1}), and N_2O saturation level (%N_2O in %) in four urban ponds (Leybeek, Pêcheries, Tenreuken, and Silex) in the city of Brussels (Belgium) from June 2021 to December 2023. Box plots show median (horizontal line), mean (cross), and 25–75% percentiles (box limits). Whiskers extend from minimum to maximum values. White and grey bands in the graphs on the right correspond to the autumn/winter and spring/summer periods, respectively, and dotted vertical bars represent the first days of each season. ANOVA results of the multiple comparison between boxplots are summarized in Table S6.

https://doi.org/10.5194/egusphere-2024-1315
Preprint. Discussion started: 14 May 2024

The $\%O_2$ values ranged from 11 to 191% (Fig. 3). The highest $\%O_2$ values in the four ponds were observed in spring and summer compared to fall and winter owing to aquatic primary production. In summer, the highest average $\%O_2$ was observed in the Leybeek pond that was characterized by the highest phytoplankton biomass as indicated by the Chl-*a* concentration. The lowest average $\%O_2$ was observed in fall in the Pêcheries pond.

The pCO_2 values ranged from 40 to 13,804 ppm (Fig. 3). Minimal values of pCO_2 were generally observed in spring and summer probably due to intense uptake of CO_2 by primary production from either phytoplankton or submerged macrophytes. Maximal pCO_2 were observed in fall probably due to release of CO_2 from degradation of organic matter due to senescence of phytoplankton or macrophytes (Fig. 3). A general control of pCO_2 by biological activity (primary production and respiration) was confirmed by the strong negative correlation with $\%O_2$ observed in all four ponds, as well as a positive correlation with DIN observed in three ponds, and a positive correlation with SRP was observed in two ponds (Table S3). A negative correlation between pCO_2 and Chl-*a* was only observed in the turbid Leybeek pond, which showed the highest average Chl-*a* concentration, and no correlation was found in clear-water ponds, where aquatic primary production was presumably mainly related to submerged macrophytes (Table S3). In all four ponds, pCO_2 strongly correlated to precipitation suggesting a control of external inputs of carbon either as organic carbon sustaining internal degradation of organic matter or as soil CO_2 (Marotta et al., 2011).

The CH_4 dissolved concentrations ranged from 194 to 48,380 nmol L^{-1} (Fig. 3). The dissolved CH_4 concentration was generally higher in spring and summer than fall and winter. Dissolved CH_4 concentration was positively correlated to water temperature in all four ponds (Table S3), most probably reflecting the increase of sedimentary methanogenesis with temperature (Schulz and Conrad, 1996). In individual ponds, dissolved CH_4 concentration was sometimes negatively correlated to precipitation, SRP, DIN, TSM, or Chl-*a* concentrations probably indirectly reflecting the seasonal variations of these variables that were minimal in summer when CH_4 was maximal presumably mainly in response to temperature increase (Table S3). A negative correlation between CH_4 and Chl-*a* was observed in the Silex pond, and a negative correlation between CH_4 and TSM was observed in the Tenreuken pond. Both are clear-water ponds where Chl-*a* or TSM concentrations were particularly low in summer (Fig. 3).

The correlations between pCO_2 and precipitation and between dissolved CH_4 concentration and temperature observed in all the four ponds individually were also observed when pooling together the data for all four ponds ("all" in Table S3). This suggested that in the four sampled ponds the effect of precipitation on pCO_2 and of temperature on dissolved CH_4 concentration outweighed other potential effects that could have arisen from differences in surface area, depth, or dominance of type of primary producers (phytoplankton or macrophyte) in explaining seasonal variations.

The $\%N_2O$ values ranged from 32 to 826% (Fig. 3). The $\%N_2O$ values did not show clear seasonal variations in any of the four sampled ponds. In individual ponds, $\%N_2O$ correlated negatively to temperature (Tenreuken) or Chl-*a* (Silex) or positively to SRP (Silex) and TSM (Tenreuken) concentrations. We do not have a clear explanation for these correlations (Table S3). The correlations with Chl-*a* and TSM were surprisingly since they were observed in the two clear-water ponds and might indirectly reflect seasonal variations (with minimal values of these two quantities in summer). More surprisingly, $\%N_2O$ was not correlated with DIN (Table S3) nor with individual forms of DIN (NH_4^+, NO_2^-, NO_3^-) in the four ponds individually. However, when all the data were pooled together, $\%N_2O$ correlated positively to DIN (Table S3), but not with individual forms of DIN (NH_4^+, NO_2^-, NO_3^-). In a previous study of the variation of GHGs in 22 urban ponds in the city of Brussels sampled only once during each season, $\%N_2O$ correlated positively with DIN, NH_4^+, NO_2^-, and NO_3^-. The range of variation of DIN and $\%N_2O$ across these 22 ponds (2 to 625 µmol L^{-1} for DIN and 0 to 10,354% for $\%N_2O$) was higher than the one observed

https://doi.org/10.5194/egusphere-2024-1315
Preprint. Discussion started: 14 May 2024

in present study of only four ponds (1 to 135 µmol L^{-1} for DIN and 32 to 826% for $\%N_2O$). The four ponds studied here are located at the periphery of the city and most probably receive less atmospheric nitrogen deposition than closer to the city center, as shown in our previous study by the correlation between $\%N_2O$ and DIN in the 22 sampled ponds and atmospheric nitrogen dioxide (Bauduin et al., 2024). Atmospheric nitrogen deposition has been shown to enhance denitrification and N_2O production in lakes (McCrackin and Elser, 2010; Palacin-Lizarbe et al., 2020).

3.2. Drivers of bubble flux

The bubble flux measured with inverted funnels in the four sampled ponds in the city of Brussels ranged between 0 and 2078 ml m^{-2} d^{-1} and strongly increased with water temperature (Fig. 4). Given the shallowness of the sampled systems (<1.5 m, Fig. 1) we assume that sediments experience the same temperature as surface waters. The CH_4 content of the bubbles also increased with bubble flux (Fig. 4). These patterns were most probably related to the strong dependence of methanogenesis on temperature (Schulz and Conrad, 1996). As temperature increases, the concomitant increase of methanogenesis leads to the build-up of gas bubbles in sediments that are richer in CH_4, and consequently to higher bubble fluxes with a higher CH_4 content.

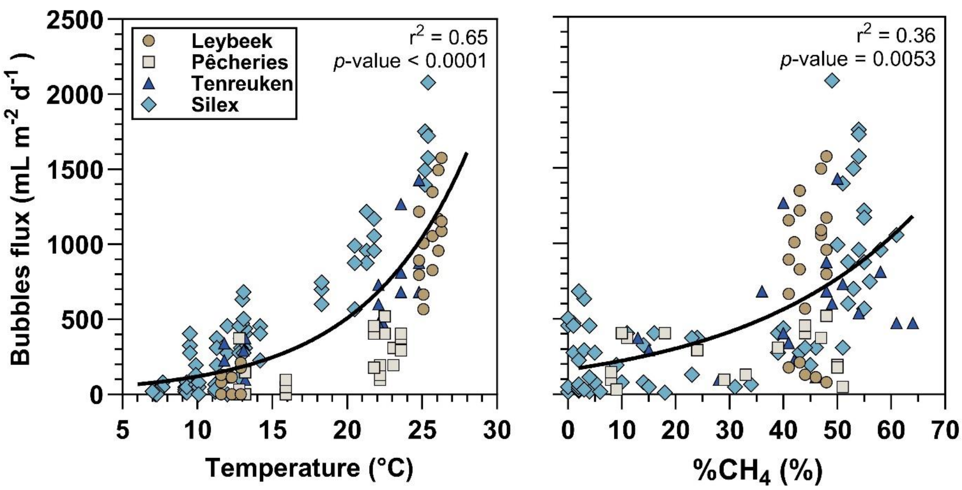

Figure 4: Bubbles flux (ml m^{-2} d^{-1}) as a function of water temperature (°C) and the relative CH_4 content in bubbles ($\%CH_4$, in %) in four urban ponds (Leybeek, Pêcheries, Tenreuken, and Silex) in the city of Brussels (Belgium). Bubbles fluxes were measured with three bubble traps in spring, summer, and fall of 2022 and 2023, totaling 8 days in the Leybeek, Pêcheries, and Tenreuken ponds and 24 days in the Silex pond. Solids lines represent exponential regression fit (Table S5).

Bubbling events are known to also be triggered by a decrease of hydrostatic pressure on the sediments due to water level fluctuations or changes in atmospheric pressure. Drops in atmospheric pressure have been documented to trigger bubble fluxes from lake sediments (Tokida et al., 2007; Scandella et al., 2011; Varadharajan and Hemond, 2012; Wik et al., 2013; Taoka et al., 2020; Zhao et al., 2021). The bubble fluxes were measured during more lengthy series at the Silex pond than the other three ponds for logistical reasons. In spring 2022, the bubble flux at the Silex pond increased during events of drops in atmospheric pressure (depressions) (Fig. 5). There was no relation between wind speed and peaks of bubble flux as shown in Gatun Lake (Keller and Stallard, 1994), suggesting a more important role of changes of atmospheric pressure than wind speed in Silex pond in spring 2022. In summer 2022, the bubble flux at the Silex pond was higher than during spring, and the temporal changes tracked those of water temperature. The bubble flux was modelled as function of temperature alone or as function of

https://doi.org/10.5194/egusphere-2024-1315
Preprint. Discussion started: 14 May 2024

both temperature and pressure changes (Figs. 5 and S3). The inclusion of the term of pressure drops in addition to temperature improved the performance of the model compared to the original data, for periods of low temperature (<15°C) but not for warmer periods (>15°C) (Figs. 5 and S3) when bubbling fluxes are quantitatively more important. The inclusion of the term of pressure changes only improved the performance of the model compared to the original data very marginally when comparing the full temperature range (<15°C and >15°C) (Fig. S3), showing that the intensity of bubble flux was mainly driven by temperature change at yearly scales.

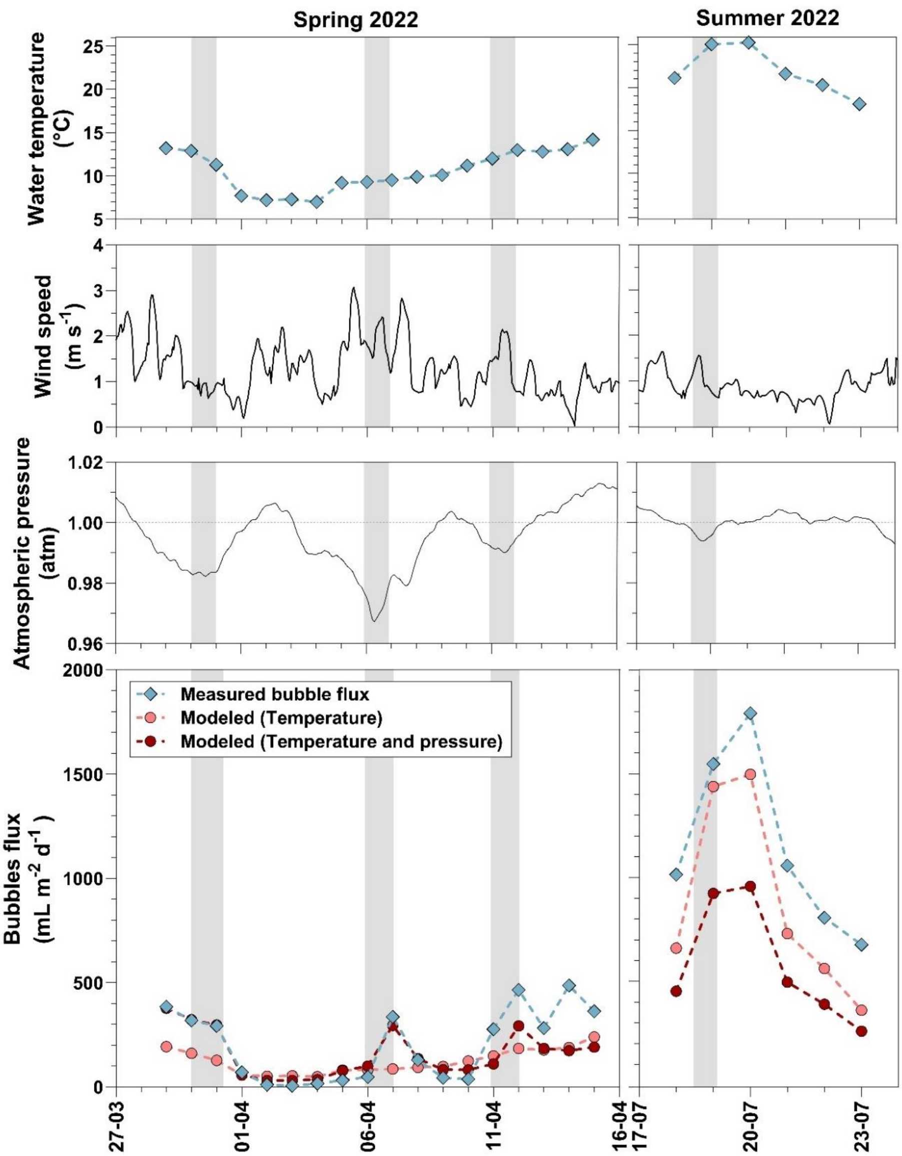

Figure 5: Water temperature (°C), wind speed (m s^{-1}), atmospheric pressure (atm), and measured and modeled bubbles flux (ml m^{-2} d^{-1}) in the Silex pond from the 29 March 2022 to the 15 April 2022 and from the 18 July 2022 to the 23 July 2022. The bubbles flux was modelled from a fit to data based on temperature alone and from both temperature and drops in atmospheric pressure.

https://doi.org/10.5194/egusphere-2024-1315
Preprint. Discussion started: 14 May 2024

3.3. Drivers of methane ebullitive fluxes

Ebullitive CH_4 fluxes in the four ponds ranged between 0 and 59 mmol m^{-2} d^{-1} and were positively related to temperature (Fig. 6) as shown previously in other systems (Wik et al., 2013; DelSontro et al., 2016; Aben et al., 2017). The fitted relations between ebullitive CH_4 fluxes and temperature were specific to each pond and encompassed the fitted relations established in similar systems: four small ponds in Québec (DelSontro et al., 2016) and a small urban pond in the Netherlands (Aben et al., 2017). The Q_{10} of CH_4 ebullition values ranged between 4.4 in the deeper Pêcheries pond and 26.9 in the shallower Leybeek pond, respectively. The Q_{10} of CH_4 ebullition in the ponds of the city of Brussels, in Québec (DelSontro et al., 2016), and in the Netherlands (Aben et al., 2017) were negatively related to water depth (Fig. 6). An increase in water temperature leads to a smaller increase in CH4 ebullitive fluxes (lower Q_{10}) in deeper ponds as the impact of hydrostatic pressure on sediments is higher in deeper ponds compared to shallow ponds, restricting bubble formation and release (DelSontro et al., 2016).

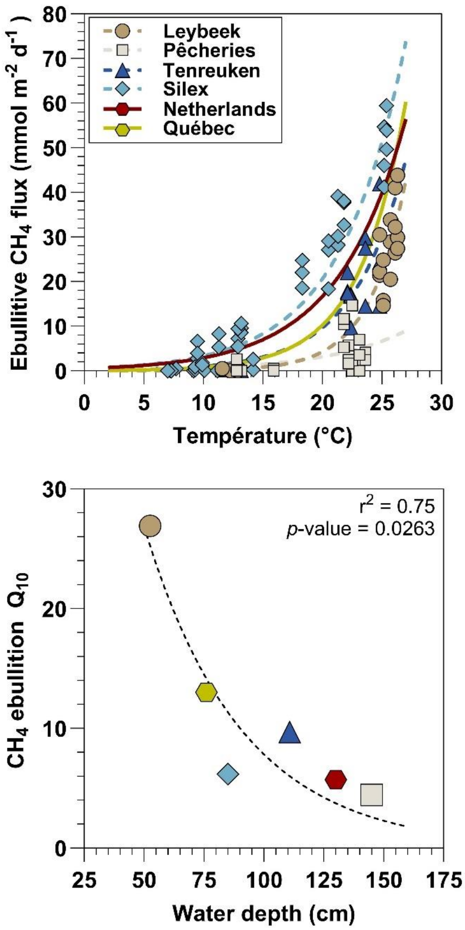

Figure 6: Measured ebullitive CH_4 fluxes (mmol m^{-2} d^{-1}) as function of water temperature (°C) in four urban ponds (Leybeek, Pêcheries, Tenreuken, and Silex) in the city of Brussels (Belgium), in spring, summer, and fall of 2022 and 2023, totaling 8 days in Leybeek, Pêcheries, and Tenreuken ponds and 24 days in Silex pond, with three bubble traps. Dashed lines represent exponential fit for the four urban ponds in the city of Brussels (Table S3) and solid lines represent exponential fit established in similar systems: four small ponds in Québec (DelSontro et al., 2016) and a small urban pond in the Netherlands (Aben et al., 2017). Each exponential curve allows to determine a Q_{10} of CH_4 ebullition, plotted against water depth, dashed line represents exponential regression fit (Table S5).

https://doi.org/10.5194/egusphere-2024-1315
Preprint. Discussion started: 14 May 2024

3.4. Relative contribution of methane ebullitive and diffusive fluxes

Diffusive CH_4 fluxes computed from CH_4 concentration and *k* derived from wind speed ranged between 0.1 and 19.7 mmol m^{-2} d^{-1} (Fig. 7). The diffusive CH_4 fluxes tended to be higher in summer and spring than in fall and winter owing to the strong positive dependency between CH_4 and water temperature (Fig. 3, Table S2). In addition, wind speed only showed small seasonal variations during sampling, ranging on average between 0.6±0.6m s^{-1} in spring, 0.3±0.2 m s^{-1} in summer, 0.7±0.7 m s^{-1} in fall and 0.6±0.2 m s^{-1} in winter (Fig. 3). Ebullitive CH_4 fluxes were calculated from the relations with temperature for each pond given in Figure 6 from the temperature data coincident with the diffusive CH_4 fluxes (Fig. 7). This allowed to compare and integrated seasonally both components of CH_4 emissions to the atmosphere, and to calculate the relative contribution of ebullition to total (diffusive+ebullitive) CH_4 emissions.

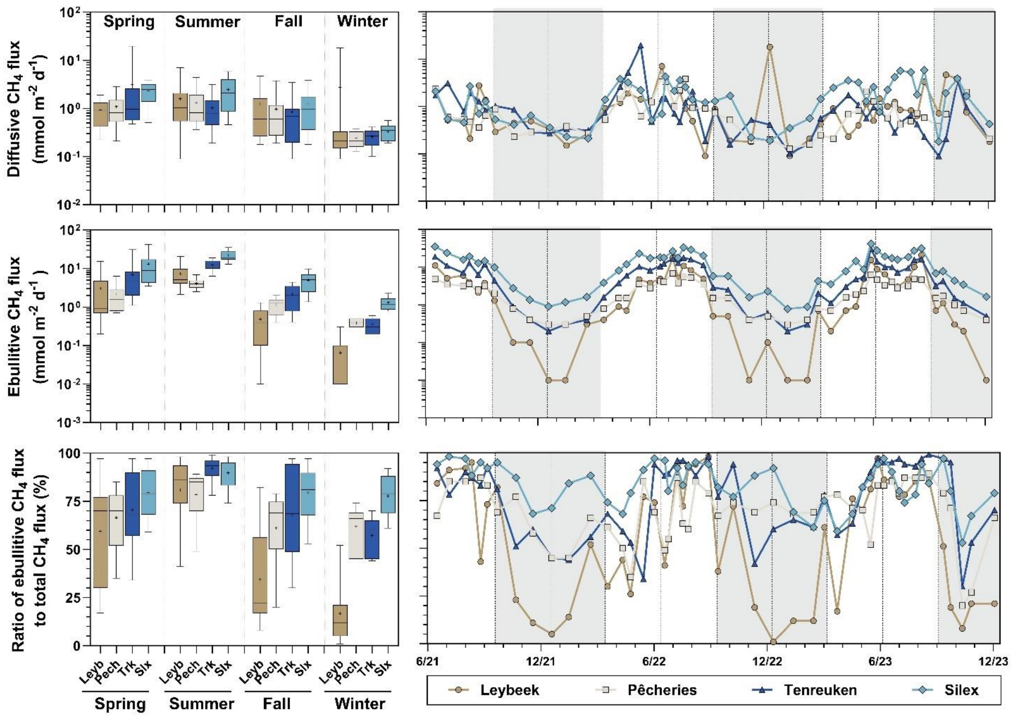

Figure 7: Seasonal variations of diffusive and ebullitive CH_4 fluxes (mmol m^{-2} d^{-1}), and the ratio of ebullitive CH_4 flux to total (ebullitve+diffusive) CH_4 flux (%) in four urban ponds (Leybeek, Pêcheries, Tenreuken, and Silex) in the city of Brussels (Belgium) from June 2021 to December 2023. Diffusive fluxes were calculated from CH_4 concentration and gas transfer velocity derived from wind speed. Ebullitive CH_4 fluxes were calculated from the relations with temperature for each pond (Table S3) from the temperature data coincident with the diffusive CH_4 fluxes. Box plots show median (horizontal line), mean (cross), and 25–75% percentiles (box limits). Whiskers extend from minimum to maximum values. White and grey bands in the graphs on the right correspond to the autumn/winter and spring/summer periods, respectively, and dotted vertical bars represent the first days of each season. ANOVA results of the multiple comparison between boxplots are summarized in Table S6.

The relative contribution of ebullition to total CH_4 emissions ranged between 1 and 99% in the four sampled ponds in the city of Brussels (Fig. 7). Owing to the strong dependency of ebullitive CH_4 fluxes to temperature (Fig. 6), the mean relative contribution of ebullition to total CH_4 emissions was highest in summer, above 75% in all ponds (Fig. 7). This is consistent with other studies showing that ebullitive CH_4 fluxes can account for more than half of total CH_4 emissions (Wik et al., 2013; Deemer and Holgerson, 2021). The relative contribution of ebullition to total CH_4 emissions was lowest during the other

https://doi.org/10.5194/egusphere-2024-1315
Preprint. Discussion started: 14 May 2024

seasons, especially in the Leybeek pond (Fig. 7). Owing to the strong dependency of ebullitive CH_4 fluxes to temperature, the relative contribution of ebullition to total CH_4 emissions was related to temperature in the four ponds (Fig. S4).

The values of Q_{10} of diffusive CH_4 fluxes were lower than those for ebullitive CH_4 fluxes, less variable (1.2 in Pêcheries to 2.9 in Silex), and less statistically significant (Table S4). Other studies have also observed higher Q_{10} for ebullitive CH_4 flux than for diffusion in lakes and ponds (DelSontro et al., 2016; Xun et al., 2024). The lower dependence to temperature of CH_4 diffusion compared to ebullition might be related to a lower relative change of CH_4 concentrations and *k* to temperature change. CH_4 concentrations in surface water are very strongly affected by MOX (see hereafter). A relative increase of CH_4 production in sediments by methanogenesis will lead to a stronger increase of CH_4 emission by ebullition than by diffusion because of a mitigation by MOX on CH_4 diffusion. Additionally, *k* depends on wind speed. The warmer periods of the year (summer) tended to be less windy (~0.3 m s^{-1}) and with lower *k* values than the other seasons (>0.6 m s^{-1}) also contributing to lower dependence of CH_4 diffusion compared to ebullition on temperature and lower Q_{10} values.

The annual averaged diffusive and ebullitive fluxes of CH_4 in the four ponds in the city of Brussels were plotted against Chl-*a* concentration, total macrophyte cover in summer, water depth, and lake surface area (Fig. 8) that are frequent predictors of variations of CH_4 fluxes among lakes (Holgerson and Raymond, 2016; DelSontro et al., 2018, Deemer and Holgerson, 2021; Casas-Ruiz et al., 2021; Borges et al., 2022). The annual diffusive and ebullitive CH_4 fluxes in the four studied ponds did not show a clear relation with depth and surface area (Fig. 8) that probably reflected the narrow range of variation of these variables (50 to 150 cm for water depth and 0.7 to 3.2 ha for lake surface area). Correlations between CH_4 fluxes and depth or lake surface area have been shown among lakes across much larger ranges of variation of lake depth (Borges et al., 2022) and surface area (Holgerson and Raymond, 2016; Casas-Ruiz et al., 2021).

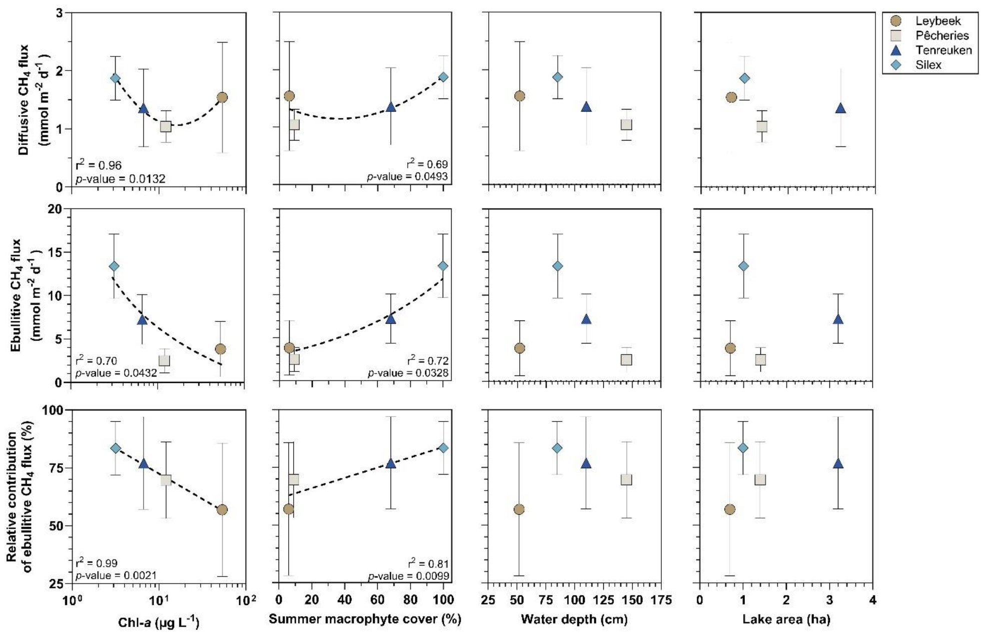

Figure 8: Mean diffusive and ebullitive CH_4 fluxes (mmol m^{-2} d^{-1}) and mean ratio of ebullitive CH_4 flux to total (diffusive+ebullitive) CH_4 flux (%) versus chlorophyll-*a* (Chl-*a*, in µg L^{-1}), total macrophyte cover in summer (%), water depth (cm), and lake surface area (ha) in four ponds (Leybeek, Pêcheries, Tenreuken, and Silex) in the city of Brussels (Belgium) from June 2021 to December 2023. Error bars indicate the standard deviation. Dashed lines indicate trends in relationship between variables (Table S5).

https://doi.org/10.5194/egusphere-2024-1315
Preprint. Discussion started: 14 May 2024

The annual ebullitive CH_4 fluxes were higher in the two clear-water lakes (Tenreuken and Silex) than the two turbid-water lakes (Leybeek and Pêcheries) and were positively correlated to macrophyte cover and negatively related to Chl-*a* (Fig. 8). This would suggest that the delivery of organic matter to sediments from macrophytes sustained a larger methane production than from phytoplankton. This is consistent with the notion that vegetated littoral zones of lakes are hot spots of CH_4 production and emission (Desrosiers et al., 2022).

The annual diffusive CH_4 flux was higher in the two clear-water lakes (Tenreuken and Silex) than in one of the turbid-water lakes (Pêcheries) which is consistent with the pattern of higher ebullitive CH_4 emissions from clear-water lakes. In the four sampled urban ponds, annual CH_4 diffusive fluxes increased in clear-water ponds with increasing total macrophyte cover and in turbid-water ponds with increasing Chl-*a* (Fig. 8). This suggests that in turbid-water lakes the methane production increases with phytoplankton biomass, as suggested in other studies (Yan et al., 2019; Bartosiewicz et al., 2021; Borges et al., 2022). Since total macrophyte cover and Chl-*a* were anti-correlated, we hypothesize that the variations of CH_4 diffusive fluxes follow a U-shaped relation with either Chl-*a* or macrophyte cover. Higher values of annual CH_4 diffusive fluxes occurred at the extreme values of Chl-*a* or macrophyte cover (minimum or maximum) and lower values occurred at the intermediate values of Chl-*a* or macrophyte cover. The relative contribution of ebullitive CH_4 fluxes to the total flux very strongly correlated positively to macrophyte cover and negatively to Chl-*a* (Fig. 8). This is consistent with the idea of an increase of ebullition relative to diffusive CH_4 emissions in vegetated sediments compared to unvegetated sediments (Desrosiers et al., 2022; Theus et al., 2023).

The annual diffusive and ebullitive fluxes in the four ponds in the city of Brussels were within the range of values for ponds of similar surface area (0.4 to 4.0 ha) compiled by Deemer and Holgerson (2021) (Fig. S5). The linear regression of ebullitive CH_4 fluxes as a function of diffusive CH_4 fluxes allows comparing the data of ebullitive CH_4 fluxes from the 4 Brussels ponds "normalized" to the diffusive CH_4 fluxes. The ebullitive CH_4 fluxes from the two turbid-water ponds (Pêcheries and Leybeek) were very close to the linear regression showing they were characterized by ebullitive CH_4 fluxes equivalent to those in the ponds compiled by Deemer and Holgerson (2021) when normalized by the diffusive fluxes. The ebullitive CH_4 fluxes from the two clear-water ponds (Tenreuken and Silex) were above the linear regression showing they were characterized by ebullitive CH_4 fluxes above those in the ponds compiled by Deemer and Holgerson (2021) when normalized by the diffusive fluxes. We hypothesize the relatively higher ebullitive fluxes in the two clear-water ponds were related to enhancement of ebullition from macrophytes. This is consistent with the two clear-water ponds in Brussels having ebullitive fluxes higher than in the ponds compiled by Deemer and Holgerson (2021) at equivalent Chl-*a* values. This would suggest that Chl-*a* concentration alone fails to predict ebullitive fluxes in macrophyte dominated clear-water ponds. Consequently, global scaling of CH_4 fluxes in lakes using Chl-*a* as a predictor (DelSontro et al. 2018) might under-estimate ebullitive CH_4 emissions due a misrepresentation of macrophyte dominated clear-water ponds.

3.5. Methanogenesis pathway inferred from $\delta^{13}C$-CH_4 in bubbles

$\delta^{13}C$-CH_4 was measured in bubbles trapped during the ebullition flux measurements and in bubbles collected by perturbing the sediments. The variations $\delta^{13}C$-CH_4 suggest that there could have been variations of the relative importance of hydrogenotrophic versus acetoclastic pathways of methanogenesis among different ponds but also seasonally. Methanogenesis by the hydrogenotrophic pathway produces CH_4 with more negative $\delta^{13}C$-CH_4 values (-100‰ to -60‰) compared to the acetoclastic pathway (-65‰ to -50‰) (Whiticar et al., 1986). Yet, it remains unclear which environmental factors determine the relative importance of hydrogenotrophic and acetoclastic methanogenesis pathways (Conrad et al., 2011).

https://doi.org/10.5194/egusphere-2024-1315
Preprint. Discussion started: 14 May 2024

The $\delta^{13}C-CH_4$ in the trapped bubbles was more negative in fall than summer and spring (Fig. 9), suggesting a dominance of hydrogenotrophic methanogenesis in fall compared to spring and summer when acetoclastic methanogenesis seemed dominant. Hydrogenotrophic methanogenesis occurs at higher temperatures than acetoclastic methanogenesis (Schulz and Conrad 1996; Schulz et al., 1997), however, temperature in fall (11.9±3.7 °C) was lower than in summer (21.1±1.9 °C). A shift from acetoclastic methanogenesis to hydrogenotrophic methanogenesis has been documented in response to the increase of NH_4^+ (Ni et al., 2022; Wang et al., 2022) and the decrease of pH (Kotsyurbenko et al., 2007) expected in response to an increase of CO_2. An increase of NH_4^+ and decrease of pH in pore waters in fall compared to summer and spring would be consistent with the sustained benthic organic matter degradation leading to a gradual change of pore water chemistry from spring to fall.

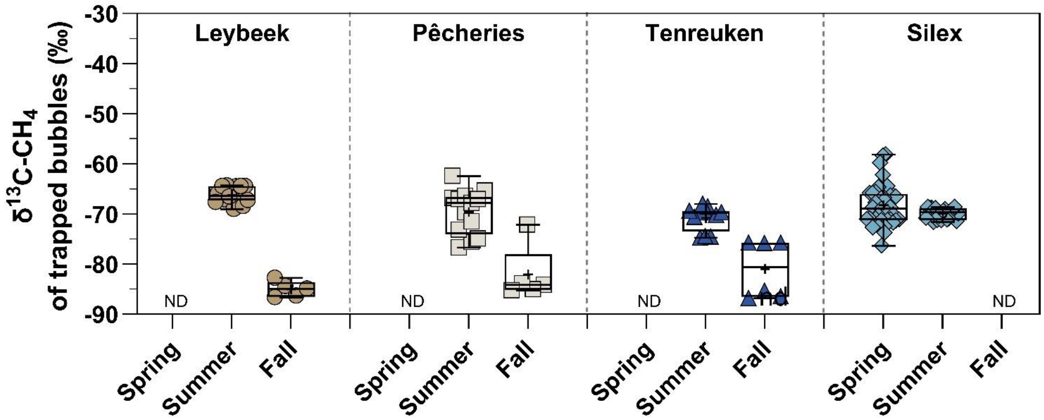

Figure 9: $^{12}C/^{13}C$ ratio of CH_4 ($\delta^{13}C-CH_4$ in ‰) in bubbles collected during ebullitive flux measurements ("trapped bubbles") in four urban ponds (Leybeek, Pêcheries, Tenreuken, and Silex) in the city of Brussels (Belgium), measured in spring, summer, and fall in 2022 and 2023 (September 2023 and October 2023 in Leybeek; July 2023 and October 2023 in Pêcheries; August 2023 and October 2023 in Tenreuken; April 2022 and July 2022 in Silex). Box plots show median (horizontal line), mean (cross), and 25–75% percentiles (box limits). Whiskers extend from minimum to maximum values. ND = no data. ANOVA results of the multiple comparison between boxplots are summarized in Table S7.

In summer 2023, a survey of all ponds was made to simultaneously sample by perturbation of the sediment for the determination of the $\delta^{13}C-CH_4$ in the released bubbles. The $\delta^{13}C-CH_4$ of perturbed sediments was more negative in the clear-water macrophyte dominated ponds than in the turbid-water phytoplankton dominated ponds (Fig. 10). This could suggest a higher contribution of the hydrogenotrophic methanogenesis pathway compared to the acetoclastic pathway in the clear-water ponds where organic matter for methanogenesis was mainly related to macrophytes rather than phytoplankton. Based on gene expression during incubations (qPCR), Wang et al., (2023) suggested that macrophyte organic carbon stimulated acetoclastic methanogenesis pathway compared to phytoplankton organic matter in lakes Chaohu and Taihu in China. The pattern of $\delta^{13}C-CH_4$ data in the four urban ponds of the city of Brussels suggests the opposite pattern, with macrophyte organic carbon stimulating the hydrogenotrophic methanogenesis pathway. This pattern seems consistent with the more refractory nature of macrophyte organic carbon compared to the more labile nature of phytoplankton organic carbon. Organic matter from macrophytes has a large share of molecules difficult to degrade such as cellulose unlike organic matter from phytoplankton that is rich in polysaccharides and proteins (West et al., 2015; Berberich et al., 2020). In presence of more refractory organic matter, a partial fermentation would favour the production of H_2 over acetate which would favour hydrogenotrophic methanogenesis over acetoclastic methanogenesis (Liu et al., 2017).

https://doi.org/10.5194/egusphere-2024-1315
Preprint. Discussion started: 14 May 2024

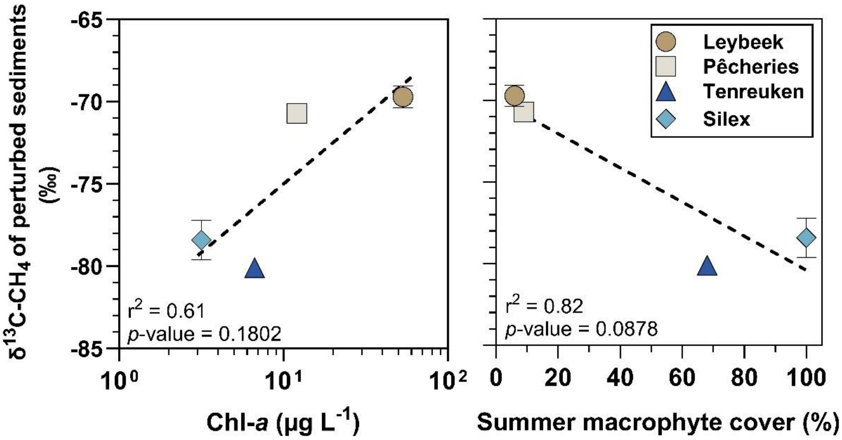

Figure 10: $^{12}C/^{13}C$ ratio of CH_4 ($\delta^{13}C$-CH_4 in ‰) in bubbles sampled after release from sediments after physical perturbation ("perturbed sediments") versus chlorophyll-*a* (Chl-*a*, in µg L^{-1}) and total macrophyte cover in summer (%) in four ponds (Leybeek, Pêcheries, Tenreuken, and Silex) in the city of Brussels (Belgium) measured in summer 2023 (4th September 2023). Error bars indicate standard deviation on the mean. Dashed lines indicate linear regressions (Table S5).

3.6. Methane oxidation

The $\delta^{13}C$-CH_4 in surface waters in the four sampled ponds in the city of Brussels ranged between -16 and -64 ‰ (Fig. 11). The $\delta^{13}C$-CH_4 in surface waters were generally higher than in sediments based on trapped bubbles during the ebullition measurements (-55 to -87 ‰; Fig. 9). The ^{13}C enriched values in surface waters samples probably resulted from MOX. FOX in surface waters in the four sampled ponds in the city of Brussels ranged between 22 and 97%. MOX in surface waters in the four sampled ponds in the city of Brussels ranged between 0.1 and 73.0 mmol m^{-2} d^{-1} (Fig. 11).

FOX and MOX followed the same seasonal variations than $\delta^{13}C$-CH_4 since both quantities were derived from isotopic models that include $\delta^{13}C$-CH_4. $\delta^{13}C$-CH_4, FOX, and MOX were in most ponds higher in summer and fall than in spring and winter (Fig. 11). $\delta^{13}C$-CH_4, FOX, and MOX showed distinct differences among the four ponds. $\delta^{13}C$-CH_4, FOX, and MOX were higher in the turbid-water ponds (Leybeek and Pêcheries) than in clear-water ponds (Tenreuken and Silex), particularly during summer (Fig. 11). $\delta^{13}C$-CH_4, FOX, and MOX positively correlated to TSM and Chl-*a* concentrations (Fig. 12). These patterns could reflect the increase of micro-organisms including methanotrophs fixed on particles leading to an increase of MOX in parallel to an increase of TSM concentration (Abril et al 2007). Micro-organisms can grow on fixed inorganic particles, aggregates of organic matter (Kirchman and Mitchell 1982), but also on aggregates of living cyanobacteria (Li et al., 2021). An increase of particles in the water column increases light attenuation in the water column which would alleviate the inhibition of MOX by light (Dumestre et al., 1999; Murase and Sugimoto 2005; Morana et al., 2020), also possibly contributing to a positive relation between MOX and TSM and Chl-*a*. Both processes could co-occur contributing to the observed positive patterns between MOX and TSM and Chl-*a* concentrations.

https://doi.org/10.5194/egusphere-2024-1315
Preprint. Discussion started: 14 May 2024

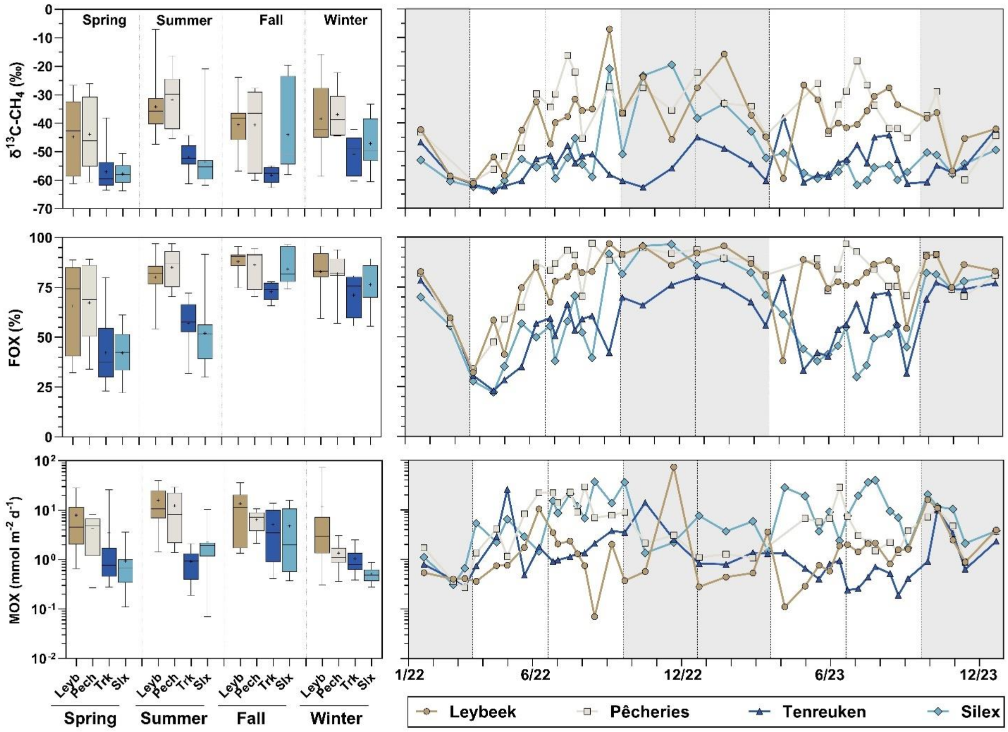

Figure 11: Seasonal variations of $^{12}C/^{13}C$ ratio of CH_4 in surface waters ($\delta^{13}C$-CH_4 in ‰), fraction of CH_4 removed by methane oxidation (FOX, in %), and methane oxidation (MOX, in mmol m^{-2} d^{-1}) in four urban ponds (Leybeek, Pêcheries, Tenreuken, and Silex) in the city of Brussels (Belgium) from January 2022 to December 2023. Box plots show median (horizontal line), mean (cross), and 25–75% percentiles (box limits). Whiskers extend from minimum to maximum values. White and grey bands in the graphs on the right correspond to the fall/winter and spring/summer periods, and dotted vertical bars represent the first days of each season. ANOVA results of the multiple comparison between boxplots are summarized in Table S6.

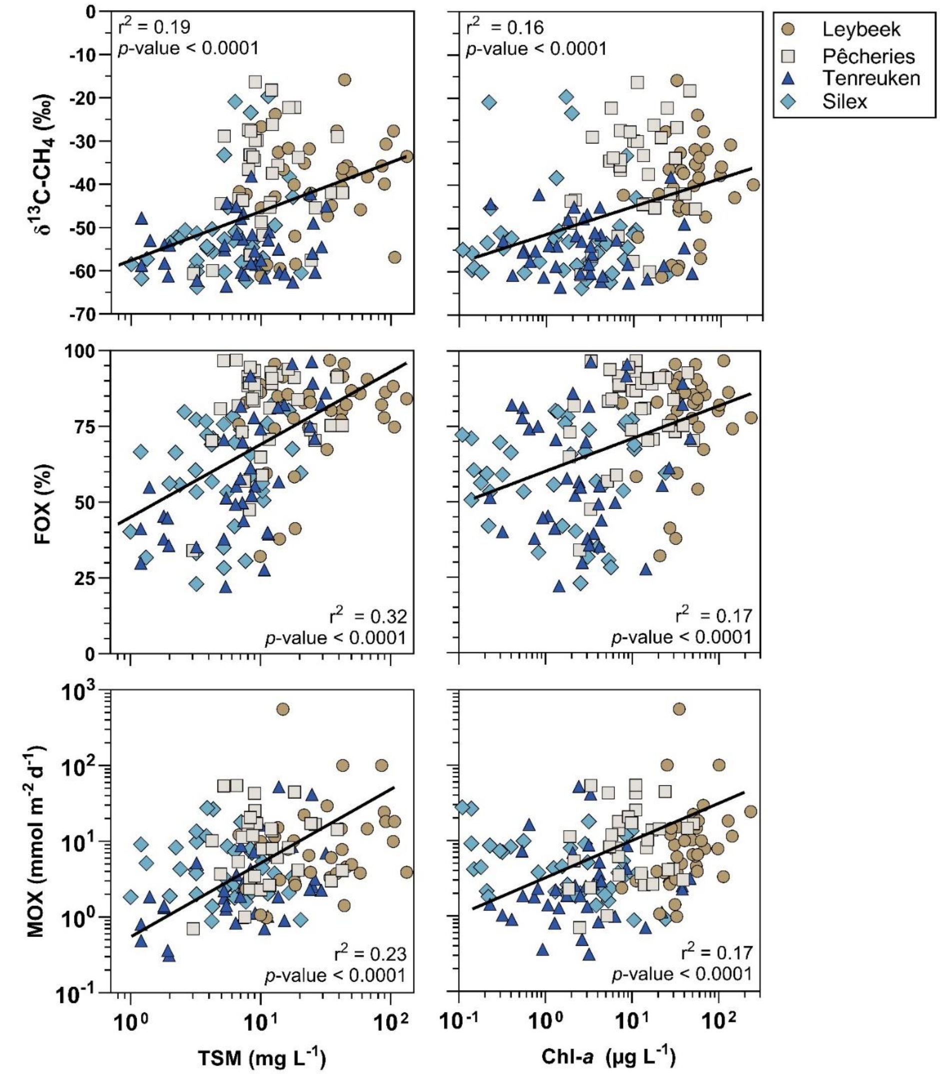

Figure 12: $^{12}C/^{13}C$ ratio of CH_4 in surface waters ($\delta^{13}C$-CH_4 in ‰), fraction of CH_4 removed by methane oxidation (FOX, in %), and methane oxidation flux (MOX, in mmol m^{-2} d^{-1}) versus total suspend matter concentration (TSM, in mg L^{-1}) and chlorophyll-*a* concentration (Chl-*a*, in µg L^{-1}) in four urban ponds (Leybeek, Pêcheries, Tenreuken, and Silex) in the city of Brussels (Belgium) from January 2022 to December 2023. Linear regression shown as black solid line (Table S5).

Figure 13 compares the main fluxes of dissolved CH_4 in the water column: MOX, diffusive CH_4 emissions, bubble dissolution that were derived from measurements, and the sedimentary diffusive CH_4 flux that was computed as a closing term (assuming a steady state) for comparative purposes. The dissolution of bubbles was a smaller input term of dissolved CH_4 compared to the diffusive sedimentary flux that represented 88±18% of the total input of CH_4 to the water column. Bubble dissolution depends on the time spent by the bubble in the water column during ascent, which is directly proportional to depth (McGinnis et al., 2006). MOX was a larger sink of dissolved CH_4 than the diffusive CH_4 emission to the atmosphere in the four ponds. For all four ponds, MOX accounted for 78±26% of total CH_4 removal from the water column, in agreement with other studies (Kankaala et al., 2006; Morana et al., 2020; Reis et al., 2022).

https://doi.org/10.5194/egusphere-2024-1315
Preprint. Discussion started: 14 May 2024

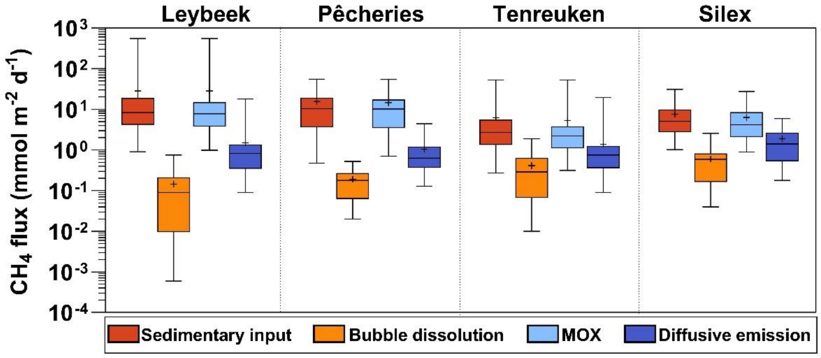

Figure 13: Bubble dissolution flux, methane oxidation (MOX), diffusive CH_4 emissions to atmosphere, and sedimentary diffusive CH_4 flux computed from the other fluxes assuming steady-state (=MOX - Bubble dissolution + atmospheric emissions) in four urban ponds (Leybeek, Pêcheries, Tenreuken, and Silex) in the city of Brussels (Belgium) between June 2021 and December 2023. All fluxes are in mmol m^{-2} d^{-1}. Box plots show median (horizontal line), mean (cross), and 25–75% percentiles (box limits). Whiskers extend from minimum to maximum values. ANOVA results of the multiple comparison between boxplots are summarized in Table S8.

3.7. Relative contribution of CO_2, CH_4 and N_2O emissions

The annual fluxes in CO_2-eq of the three GHGs (CO_2, CH_4, and N_2O) in 2022 and 2023 were higher in the two clear-water ponds than in the two turbid-water ponds (Fig. 14) due to higher CH_4 emissions (diffusive+ebullitive) in clear ponds than in turbid ponds, as there were no significant differences between the four ponds for CO_2 et N_2O emissions in 2022 and 2023.

The majority of GHG emissions in CO_2-eq was related to CO_2 and CH_4 (diffusive+ebullitive) in the four ponds. In turbid-water ponds CO_2 represented the largest fraction of GHG emissions (68.5% (2022) and 79.3% (2023), and 49.0 (2022) and 58.3 (2023) in Pêcheries and Leybeek ponds, respectively), and in clear-water ponds CH_4 represented the largest fraction of GHG emissions (66.5 (2022) and 63.3 (2023), and 60.8% (2022) and 50.0% (2023), in Silex and Tenreuken ponds, respectively). The higher annual GHG emissions in CO_2-eq from the two clear-water ponds than the turbid-water ponds were related to the higher contribution of ebullitive CH_4 fluxes. N_2O contribution to GHG emissions was marginal and ranged between 0.0% in the Pêcheries pond that occasionally acts as a sink and 1.7% in the Leybeek pond.

The GHG fluxes peaked seasonally in summer with 2.9 and 1.7 mg CO_2-eq m^{-2} d^{-1} in the Silex and the Tenreuken ponds, respectively, and 1.1 mg CO_2-eq m^{-2} d^{-1} in the Leybeek pond. The GHG fluxes peaked in fall in the Pêcheries, with 1.3 mg CO_2-eq m^{-2} d^{-1}. The higher value of the total GHG emissions in fall compared to other seasons in the Pêcheries pond is due to the summer increase in CH_4 was lower than the CO_2 increase in fall, which particularly increased in fall 2023. The GHG fluxes were the lowest in winter with 1.3 and 0.9 mg CO_2-eq m^{-2} d^{-1} in the Silex and the Tenreuken ponds, respectively, and 0.8 and 0.6 mg CO_2-eq m^{-2} d^{-1} in the Pêcheries and the Leybeek ponds, respectively. The relative contribution of ebullitive CH_4 fluxes peaked in summer in all four ponds, 73.8% and 70.9% in the Silex and the Tenreuken ponds, respectively, and 23.6% and 58.3% in the Pêcheries and the Leybeek ponds, respectively. The relative contribution of ebullitive CH_4 fluxes was lowest in winter with 22.1% and 10.0% in the Silex and the Tenreuken ponds, respectively, and 6.7% and 1.0% in the Pêcheries and the Leybeek ponds, respectively.

https://doi.org/10.5194/egusphere-2024-1315
Preprint. Discussion started: 14 May 2024

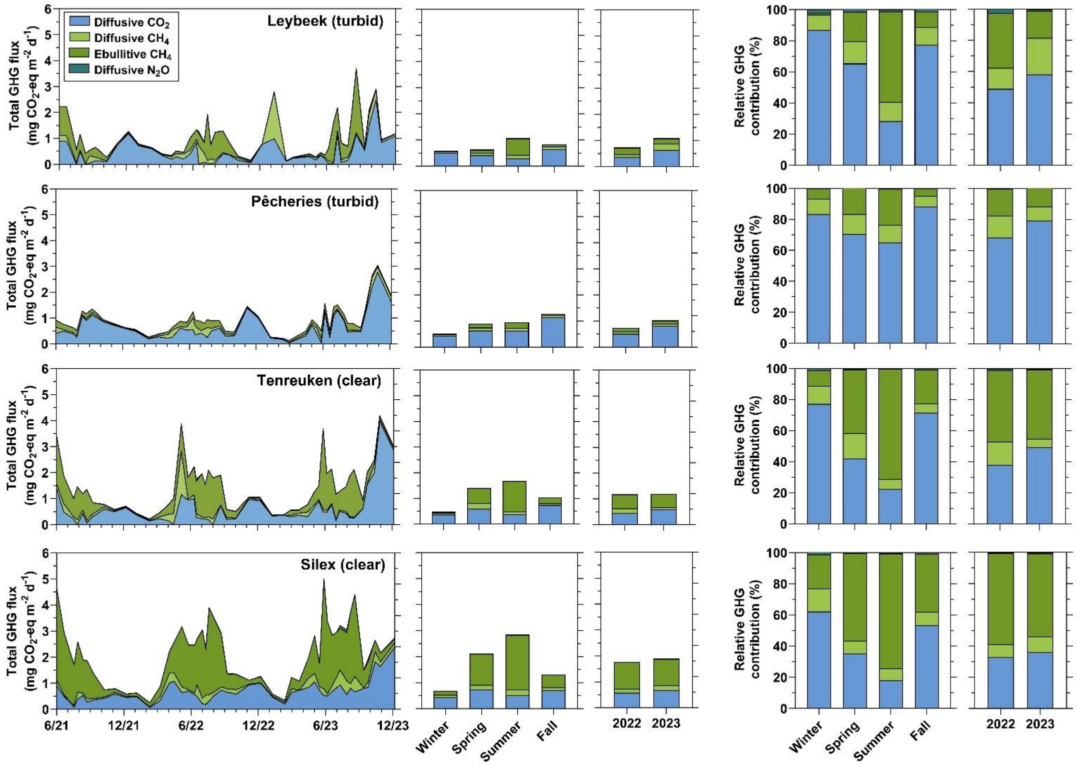

Figure 14: Temporal evolution and relative contribution of emissions to the atmosphere of CO_2 (diffusive), CH_4 (diffusive and ebullitive), and N_2O (diffusive) expressed in CO_2 equivalents (in mg CO_2-eq m^{-2} d^{-1}), in four urban ponds (Leybeek, Pêcheries, Tenreuken, and Silex) in the city of Brussels (Belgium) from June 2021 to December 2023. Averages per season include data from 2021, 2022, and 2023. Year 2023 had a higher annual precipitation (1011 mm) than year 2022 (701 mm).

The annual GHG fluxes increased from 2022 to 2023 due to an increase in relative contribution of CO_2 diffusive emissions in all four ponds. CO_2 diffusive emissions averaged 0.5 mg CO_2 m^{-2} d^{-1} in 2022 and 0.7 mg CO_2 m^{-2} d^{-1} in 2023. CO_2 emissions were two times higher in summer 2023 than in summer 2022, and 2.5 times higher in fall 2023 than in fall 2022, for similar values between 2023 and 2022 in spring and winter (1.1 higher and 1.1 lower, respectively). Spring, summer and fall were rainier in 2023 than 2022 (2.2, 2.5 and 1.4 times, respectively) and winter 2023 was 1.2 times drier than winter 2022. Winter, spring and summer were colder in 2023 than in 2022 (-0.5, -1.1°C and -0.4°C, respectively), and fall was warmer in 2023 than 2022 (+0.6°C). Higher precipitations are likely to increase the inputs of organic and inorganic carbon from soils to ponds by ground-waters, soil-waters, and surface runoff, as previously shown in other lakes (Marotta et al., 2011). Higher runoff combined with higher temperature led to more favourable conditions for OM degradation and respiration. The highest seasonal increase of CO_2 emissions was observed in fall 2023 (rainier and warmer in 2023 than in 2022), followed by summer and spring, which showed the higher decrease of temperature in 2023 compared to 2022. While this hypothesis is only based on the comparison of two years, the increase of the relative contribution of CO_2 diffusive emissions was observed in all four ponds which suggests a common uniform driver that would be consistent with a large variation weather such as annual precipitation. The El Niño event in 2023 has induced low-level cyclonic wind anomalies and higher precipitation over Western Europe, including Belgium (Chen et al., 2024).

https://doi.org/10.5194/egusphere-2024-1315
Preprint. Discussion started: 14 May 2024

4. Conclusions

We found very marked differences in CH_4 dynamics between the two clear-water macrophyte dominated ponds (Tenreuken and Silex) and the two turbid-water phytoplankton dominated ponds (Pêcheries and Leybeek) of the city of Brussels. MOX was more important in the two turbid-water ponds compared to the clear-water ponds. MOX correlated to TSM and Chl-*a* concentrations possibly owing to a higher abundance of methanotrophs in the water column fixed to particles and/or an attenuation of light limitation of MOX. Ebullitive CH_4 emissions were higher in the two clear-water ponds than the two turbid-water ponds, possibly related to high availability of macrophyte organic matter. The annual diffusive N_2O and CO_2 fluxes in 2022-2023 were not statistically different in the two clear-water ponds (Tenreuken and Silex) and in the two turbid-water ponds (Pêcheries and Leybeek). Other studies have found no difference in N_2O sedimentary production in lakes with high and low density of submerged macrophytes. We hypothesize that in human impacted system such as the urban ponds in the city of Brussels, the strong range of variations of DIN was the main driver of N_2O levels and over-rides other possible drivers such as presence or absence of macrophytes. Such a hypothesis was consistent with an overall positive relation between %N_2O and DIN in the urban ponds of the city of Brussels irrespective of presence or absence of macrophytes (Bauduin et al., 2024; this study).

The total (diffusive and ebullitive) CH_4 emissions represented 57.7±28.9% (ranging from 4.9 to 99.9%) of total GHG emissions in CO_2 equivalents in the two clear-water ponds compared to 41.0±28.7% (ranging from 2.8 to 99.9%) in two turbid-water ponds. CO_2 represented nearly all the remainder of total GHG emissions, since N_2O represented a very marginal fraction (0.8±1.6%, ranging from 0.0% to 14.9%, with the maximum coinciding with minimal total GHG flux in the Leybeek pond). The seasonal variations of GHG emissions were dominated by ebullitive seasonal variations that peaked in summer (both quantitatively and relatively), as CH_4 ebullition was strongly related to temperature. The pCO_2 values in the four sampled ponds increased with precipitation at seasonal scale, probably in relation to higher inputs of organic and inorganic carbon by surface runoff. Years 2022 and 2023 were abnormally dry and wet, respectively. This seemed to have affected the GHG emissions that were higher in 2023 mainly due to an increase in the relative contribution of CO_2 emissions, probably in response to a strong El Niño event. This would suggest that variations of precipitation also affected year-to-year variations of CO_2 emissions in addition to partly regulating seasonal variations of CO_2 emissions from the studied ponds.

Data availability. Full timestamped and georeferenced data-set is available at 10.5281/zenodo.11103556.

Author contributions. AVB and NG conceived the study; TB collected field samples; TB and AVB made the laboratory analysis; TB and AVB jointly interpreted data and drafted the manuscript with substantial inputs from NG.

Competing interests. The authors declare that they have no conflict of interest.

Acknowledgements. We thank Ozan Efe (University of Liège) and Adriana Anzil (Free University of Brussels) for analytical assistance, Florence Charlier (Free University of Brussels) for help in macrophyte identification and density quantification (Table S1), Bruxelles Environnement for providing information on history of operations in the ponds (Table S2), and Cédric Morana for help and advice in setting up the Picarro G2201-i isotopic analyzer. AVB is a Research Director at the FRS-FNRS.

Financial support. TB received funding from the Brussels-Capital Region’s institute for the encouragement of scientific research and innovation (Innoviris) as part of the Smartwater project (RBC/2020-EPF-6 h) and from the “Fonds pour la formation à la Recherche dans l’Industrie et dans l’Agriculture” (FRIA, Belgium). The Picarro G2201-i isotopic analyzer was funded by FRS-FNRS (U.N005.21).

References

Aben, R. C. H., Barros, N., Van Donk, E., Frenken, T., Hilt, S., Kazanjian, G., Lamers, L. P. M., Peeters, E. T. H. M., Roelofs, J.G.M., de Senerpont Domis, L. S., Stephan, S., Velthuis, M., Van de Waal, D., Wik, M., Thornton, B., Wilkinson, J., Delsontro, T., and Kosten, S.: Cross continental increase in methane ebullition under climate change. *Nature communications*, *8*(1), 1682. https://doi.org/10.1038/s41467-017-01535-y, 2017.

Abril, G., Commarieu, M. V., and Guérin, F.: Enhanced methane oxidation in an estuarine turbidity maximum. *Limnology and oceanography*, *52*(1), 470-475. https://doi.org/10.4319/lo.2007.52.1.0470, 2007.

Audet, J., Carstensen, M.V., Hoffmann, C.C., Lavaux, L., Thiemer, K., and Davidson, T.A.: Greenhouse gas emissions from urban ponds in Denmark. Inland Waters 10 (3), 373–385. https://doi.org/10.1080/20442041.2020.1730680, 2020.

Baliña, S., Sanchez, M. L., Izaguirre, I., and del Giorgio, P. A.: Shallow lakes under alternative states differ in the dominant greenhouse gas emission pathways. Limnology and Oceanography, 68(1), 1-13. https://doi.org/10.1002/lno.12243,2023.

Barko, J. W., Gunnison, D., and Carpenter, S. R.: Sediment interactions with submersed macrophyte growth and community dynamics. *Aquatic botany*, *41*(1-3), 41-65. https://doi.org/10.1016/0304-3770(91)90038-7, 1991.

Bartosiewicz, M., Maranger, R., Przytulska, A., and Laurion, I.: Effects of phytoplankton blooms on fluxes and emissions of greenhouse gases in a eutrophic lake. *Water Research*, *196*, 116985. https://doi.org/10.1016/j.watres.2021.116985, 2021.

Bastviken D., Ejlertsson J. and Tranvik L.: Measurement of methane oxidation in lakes: A comparison of methods. Environmental Science & Technology, 36, 3354-3361. https://doi.org/10.1021/es010311p, 2002.

Bastviken, D., Cole, J., Pace, M., and Tranvik, L.: Methane emissions from lakes: Dependence of lake characteristics, two regional assessments, and a global estimate. *Global biogeochemical cycles*, *18*(4). https://doi.org/10.1029/2004GB002238, 2004.

Bastviken, D., Treat, C.C., Pangala, S.R., Gauci, V., Enrich-Prast, A., Karlson, M., Gålfalk, M., Romano, M.B., and Sawakuchi, H.O.: The importance of plants for methane emission at the ecosystem scale. Aquat Bot 184, 103596. https://doi.org/10.1016/j.aquabot.2022.103596, 2023.

Bauduin, T., Gypens, N., and Borges, A. V.: Seasonal and spatial variations of greenhouse gas (CO_2, CH_4 and N_2O) emissions from urban ponds in Brussels. *Water Research*, 121257. https://doi.org/10.1016/j.watres.2024.121257, 2024.

Berberich, M. E., Beaulieu, J. J., Hamilton, T. L., Waldo, S., and Buffam, I.: Spatial variability of sediment methane production and methanogen communities within a eutrophic reservoir: importance of organic matter source and quantity. Limnol. Oceanogr. 65, 1–23. https://doi.org/10.1002/lno.11392, 2020.

Borges, A.V., Darchambeau, F., Lambert, T., Morana, C., Allen, G.H., Tambwe, E., and Bouillon, S.: Variations in dissolved greenhouse gases (CO_2, CH_4, N_2O) in the Congo River network overwhelmingly driven by fluvial-wetland connectivity. Biogeosciences 16 (19), 3801–3834. https://doi.org/10.5194/bg-16-3801-2019, 2019.

Borges, A.V., Deirmendjian, L., Bouillon, S., Okello, W., Lambert, T., Roland, F.A.E., Razanamahandry, V.F., Voarintsoa, N.R.G., Darchambeau, F., Kimirei, I.A., Descy, J., Allen, G.H., and Morana, C.: Greenhouse gas emissions from African lakes are no longer a blind spot. Sci. Adv. 8 (25), eabi8716. https://doi.org/10.1126/sciadv. abi8716, 2022.

Brans, K.I., Engelen, J.M., Souffreau, C., and De Meester, L.: Urban hot-tubs: local urbanization has profound effects on average and extreme temperatures in ponds. Landsc. Urban Plan. 176, 22–29. https://doi.org/10.1016/j, 2018.

Cael, B. B., Heathcote, A. J., and Seekell, D. A.: The volume and mean depth of Earth's lakes. *Geophysical Research Letters*, *44*(1), 209-218. https://doi.org/10.1002/2016GL071378, 2017.

Casas-Ruiz, J.P., Jakobsson, J., and del Giorgio, P.A.: The role of lake morphometry in modulating surface water carbon concentrations in boreal lakes. Environ. Res. Lett. 16 (7), 074037 https://doi.org/10.1088/1748-9326/ac0be3, 2021.

Chen, B., Zhang, L., and Wang, C.: Distinct impacts of the central and eastern Atlantic Niño on the European climate. Geophysical Research Letters, 51(2), e2023GL107012. https://doi.org/10.1029/2023GL107012, 2024.

Choudhury, M. I., McKie, B. G., Hallin, S., and Ecke, F.: Mixtures of macrophyte growth forms promote nitrogen cycling in wetlands. *Science of the Total Environment*, *635*, 1436-1443. https://doi.org/10.1016/j.scitotenv.2018.04.193, 2018.

Clifford, C.C., and Heffernan, J.B.: Artificial aquatic ecosystems. Water 10 (8), 1096. https://doi.org/10.3390/w10081096, 2018.

Cole, J.J., and Caraco, N.F.: Atmospheric exchange of carbon dioxide in a low-wind oligotrophic lake measured by the addition of SF_6. Limnol. Oceanogr. 43 (4), 647–656. https://doi.org/10.4319/lo.1998.43.4.0647, 2018.

https://doi.org/10.5194/egusphere-2024-1315
Preprint. Discussion started: 14 May 2024

Coleman, D. D., Risatti, J. B., and Schoell, M.: Fractionation of carbon and hydrogen isotopes by methane oxidizing bacteria. Geochimica Cosmochimica Acta, 45, 1033–1037. https://doi.org/10.1016/0016-7037(81)90129-0, 1981.

Conrad, R., Noll, M., Claus, P., Klose, M., Bastos, W. R., and Enrich-Prast, A.: Stable carbon isotope discrimination and microbiology of methane formation in tropical anoxic lake sediments. *Biogeosciences*, *8*(3), 795-814. https://doi.org/10.5194/bg-8-795-2011, 2011.

Dan, Z., Chuan, W., Qiaohong, Z., and Xingzhong, Y.: Sediments nitrogen cycling influenced by submerged macrophytes growing in winter. *Water Science and Technology*, *83*(7), 1728-1738. https://doi.org/10.2166/wst.2021.081, 2021.

Davidson, T.A., Audet, J., Svenning, J.C., Lauridsen, T.L., Søndergaard, M., Landkildehus, F., and Jeppesen, E.: Eutrophication effects on greenhouse gas fluxes from shallow-lake mesocosms override those of climate warming. Glob. Chang. Biol. 21 (12), 4449–4463. https://doi.org/10.1111/gcb.13062, 2015.

Deemer, B. R., and Holgerson, M. A.: Drivers of methane flux differ between lakes and reservoirs, complicating global upscaling efforts. *Journal of Geophysical Research: Biogeosciences*, *126*(4) https://doi.org/10.1029/2019JG005600

DelSontro, T., Beaulieu, J. J., and Downing, J. A. (2018). Greenhouse gas emissions from lakes and impoundments: Upscaling in the face of global change. *Limnology and Oceanography Letters*, *3*(3), 64-75. https://doi.org/10.1002/lol2.10073, 2021.

DelSontro, T., L. Boutet, A. St-Pierre, P.A. del Giorgio, and Y.T.: Prairie, Methane ebullition and diffusion from northern ponds and lakes regulated by the interaction between temperature and system productivity, Limnol. Oceanogr. 61(S1), S62-S77 https://doi.org/10.1002/lno.10335, 2016.

DelSontro, T., Kunz, M. J., Kempter, T., Wüest, A., Wehrli, B., and Senn, D. B.: Spatial Heterogeneity of Methane Ebullition in a Large Tropical Reservoir, Environmental Science & Technology 45 (23), 9866-9873, https://doi.org/10.1021/es2005545, 2011.

Deng, Hg., Zhang, J., Wu, Jj., Yao, X., and Yang, L.-W.: Biological denitrification in a macrophytic lake: implications for macrophytes-dominated lake management in the north of China. Environ Sci Pollut Res 27, 42460–42471. https://doi.org/10.1007/s11356-020-10230-3 , 2020.

Desrosiers, K., DelSontro, T., and del Giorgio, P. A.: Disproportionate Contribution of Vegetated Habitats to the CH4 and CO2 Budgets of a Boreal Lake. *Ecosystems*, 1-20. https://doi.org/10.1007/s10021-021-00730-9, 2022.

Dumestre, J. F., Guézennec, J., Galy-Lacaux, C., Delmas, R., Richard, S., and Labroue, L.: Influence of light intensity on methanotrophic bacterial activity in Petit Saut Reservoir, French Guiana. *Applied and environmental microbiology*, *65*(2), 534-539., https://doi.org/10.1128/aem.65.2.534-539.1999, 1999.

Dutton, G., Elkins II, J., Hall, B., NOAA ESRL, Earth System Research Laboratory Halocarbons and Other Atmospheric Trace Gases Chromatograph for Atmospheric Trace Species (CATS) Measurements. NOAA National Centers for Environmental Information. https://doi.org/10.7289/V5X0659V. Version 1. [Database: atmospheric nitrous oxide N2O] [2024-03–27], 2017.

Gorsky, A.L., Racanelli, G.A., Belvin, A.C., and Chambers, R.M.: Greenhouse gas flux from stormwater ponds in southeastern Virginia (USA). Anthropocene 28, 100218. https://doi.org/10.1016/j.ancene.2019.100218, 2019.

Grasshoff, K., and Johannsen, H.: A new sensitive and direct method for the automatic determination of ammonia in sea water. ICES J. Mar. Sci. 34 (3), 516–521. https://doi.org/10.1093/icesjms/34.3.516, 1972.

Grasshoff, K., Kremling, K., and Ehrhardt, M.: Methods of Seawater Analysis: Determination of Nitrite. John Wiley & Sons, 2009.

Greinert J., and D.F. McGinnis: Single bubble dissolution model – The graphical user interface SiBu-GUI, Environmental Modelling & Software, 24, 1012-1013, https://doi.org/10.1016/j.envsoft.2008.12.011, 2009.

Grinham, A., Albert, S., Deering, N., Dunbabin, M., Bastviken, D., Sherman, B., Lovelock, C.E., and Evans, C.D.: The importance of small artificial water bodies as sources of methane emissions in Queensland, Australia. Hydrol. Earth Syst. Sci. 22 (10), 5281–5298. https://doi.org/10.5194/hess-22-5281-2018, 2018.

Harpenslager, S. F., Thiemer, K., Levertz, C., Misteli, B., Sebola, K. M., Schneider, S. C., Hilt, S., and Köhler, J.: Short-term effects of macrophyte removal on emission of CO2 and CH4 in shallow lakes. *Aquatic Botany*, *182*, 103555. https://doi.org/10.1016/j.aquabot.2022.103555, 2022.

Herrero Ortega, S., Romero Gonz´alez-Quijano, C., Casper, P., Singer, G.A., and Gessner, M.O.: Methane emissions from contrasting urban freshwaters: rates, drivers, and a whole-city footprint. Glob. Chang. Biol. 25 (12), 4234–4243. https://doi.org/10.1111/gcb.14799, 2019.

Hilt, S., Brothers, S., Jeppesen, E., Veraart, A. J., and Kosten, S.: Translating regime shifts in shallow lakes into changes in ecosystem functions and services. *BioScience*, *67*(10), 928-936. https://doi.org/10.1093/biosci/bix106,2017.

Holgerson, M., and Raymond, P.: Large contribution to inland water CO2 and CH4 emissions from very small ponds. Nat. Geosci. 9, 222–226. https://doi.org/10.1038/ngeo2654, 2016.

Johnson, M.S., Matthews, E., Du, J., Genovese, V., and Bastviken, D.: Methane Emission from Global Lakes: New Spatiotemporal Data and Observation-Driven Modeling of Methane Dynamics Indicates Lower Emissions. Journal of Geophysical Research: Biogeosciences, 127(7). https://doi.org/10.1029/2022JG006793, 2022.

Kankaala, P., Huotari, J., Peltomaa, E., Saloranta, T., and Ojala, A.: Methanotrophic activity in relation to methane efflux and total heterotrophic bacterial production in a stratified, humic, boreal lake. *Limnology and Oceanography*, *51*(2), 1195-1204. https://doi.org/10.4319/lo.2006.51.2.1195, 2006.

Keller, M., and R. F. Stallard: Methane emission by bubbling from Gatun Lake, Panama, J. Geophys. Res., 99(D4), 8307–8319, doi:10.1029/92JD02170, 1994.

Kelly, C. A., and Chynoweth, D. P.: The contributions of temperature and of the input of organic matter in controlling rates of sediment methanogenesis 1. *Limnology and Oceanography*, *26*(5), 891-897. https://doi.org/10.4319/lo.1981.26.5.0891, 1981.

Kirchman D., and Mitchell, R.: Contribution of Particle-Bound Bacteria to Total Microheterotrophic Activity in Five Ponds and Two Marshes, Applied And Environmental Microbiology, 43, 200-209, https://doi.org/10.1128/aem.43.1.200-209.1982, 1982.

Koroleff, J.: Determination of total phosphorus by alkaline persulphate oxidation. Methods of Seawater Analysis. Verlag Chemie, Wienheim, pp. 136–138, 1983.

Kotsyurbenko, O. R., Friedrich, M. W., Simankova, M. V., Nozhevnikova, A. N., Golyshin, P. N., Timmis, K. N., and Conrad, R.: Shift from acetoclastic to H2-dependent methanogenesis in a West Siberian peat bog at low pH values and isolation of an acidophilic Methanobacterium strain. *Applied and Environmental Microbiology*, *73*(7), 2344-2348. https://doi.org/10.1128/AEM.02413-06, 2007.

Lauerwald, R., Regnier, P., Figueiredo, V., Enrich-Prast, A., Bastviken, D., Lehner, B., Maavara, T., and Raymond, P.: Natural Lakes Are a Minor Global Source of N2O to the Atmosphere. *Global Biogeochemical Cycles, 33(12),* 1564–1581. https://doi.org/10.1029/2019GB006261, 2019.

Lauerwald, R., Allen, G. H., Deemer, B. R., Liu, S., Maavara, T., Raymond, P., Alcott, L., Bastviken, D., Hastie, A., Holgerson, M.A., Johnson, M. S., Lehner, B., Lin, P., Marzadri, A., Ran, L., Tian, H., Yang, X., Yao, Y., and Regnier, P.: Inland water greenhouse gas budgets for RECCAP2: 2. Regionalization and homogenization of estimates. Global Biogeochemical Cycles, 37, e2022GB007658. https://doi.org/10.1029/2022GB007658, 2023.

Li, C., Hambright, K. D., Bowen, H. G., Trammell, M. A., Grossart, H. P., Burford, M. A., Hamilton, D.P., Jiang, H., Latour, D., Meyer, E. I., Padisák, J., Zamor, R. M. and Krumholz, L. R.: Global co-occurrence of methanogenic archaea and methanotrophic bacteria in Microcystis aggregates, *Environmental Microbiology*, *23*(11)https://doi.org/10.1111/1462-2920.15691, 2021.

Liptay, K., Chanton, J., Czepiel, P., and Mosher, B.: Use of stable isotopes to determine methane oxidation in landfill cover soils. *Journal of Geophysical Research: Atmospheres*, *103*(D7), 8243-8250. https://doi.org/10.1029/97JD02630, 1998.

Liu, Y., Conrad, R., Yao, T., Gleixner, G., and Claus, P.: Change of methane production pathway with sediment depth in a lake on the Tibetan plateau. *Palaeogeography, Palaeoclimatology, Palaeoecology*, *474*, 279-286. https://doi.org/10.1016/j.palaeo.2016.06.021, 2017.

Maavara, T., Lauerwald, R., Laruelle, G. G., Akbarzadeh, Z., Bouskill, N. J., Van Cappellen, P., and Regnier, P.: Nitrous oxide emissions from inland waters: Are IPCC estimates too high? Global Change Biology, 25(2), 473–488. https://doi.org/10.1111/gcb.145042, 2019.

Marotta, H., Duarte, C. M., Pinho, L., and Enrich-Prast, A.: Rainfall leads to increased pCO2 in Brazilian coastal lakes. *Biogeosciences*, *7*(5), 1607-1614. https://doi.org/10.5194/bg-7-1607-2010 , 2010.

Martinez-Cruz, K., Gonzalez-Valencia, R., Sepulveda-Jauregui, A., Plascencia- Hernandez, F., Belmonte-Izquierdo, Y., and Thalasso, F.: Methane emission from aquatic ecosystems of Mexico City. Aquat. Sci. 79, 159–169. https://doi.org/10.1007/s00027-016-0487-y, 2017.

McCrackin, M.L., and Elser, J. J.: Atmospheric nitrogen deposition influences denitrification and nitrous oxide production in lakes, Ecology, 91(2):528-39. https://doi.org/10.1890/08-2210.1, 2010.

McGinnis, D.F., Greinert, J., Artemov, Y., Beaubien, S.E., and Wüest, A.: The fate of rising methane bubbles in stratified waters: what fraction reaches the atmosphere? Journal of Geophysical Research 111, C09007. https://doi.org/10.1029/2005JC003183, 2006.

Morana, C., Bouillon, S., Nolla-Ardèvol, V., Roland, F. A., Okello, W., Descy, J. P., Nankabirwa, A., Nabafu, E., Springael, D., and Borges, A. V.: Methane paradox in tropical lakes? Sedimentary fluxes rather than pelagic production in oxic conditions sustain methanotrophy and emissions to the atmosphere, Biogeosciences, 17, 5209-5221, https://doi.org/10.5194/bg-17-5209-2020, 2020.

https://doi.org/10.5194/egusphere-2024-1315
Preprint. Discussion started: 14 May 2024

Morana C., Borges A.V., Roland F.A.E., Darchambeau F., Descy J.-P. and Bouillon S.: Methanotrophy within the water column of a large meromictic tropical lake (Lake Kivu, East Africa). Biogeosciences, 12, 2077-2088. https://doi.org/10.5194/bg-12-2077-2015, 2015.

Murase, J., and Sugimoto, A.: Inhibitory effect of light on methane oxidation in the pelagic water column of a mesotrophic lake (Lake Biwa, Japan). *Limnology and oceanography*, *50*(4), 1339-1343. https://doi.org/10.4319/lo.2005.50.4.1339, 2005.

Natchimuthu, S., Panneer Selvam, B., and Bastviken, D.: Influence of weather variables on methane and carbon dioxide flux from a shallow pond. Biogeochemistry 119, 403–413. https://doi.org/10.1007/s10533-014-9976-z, 2014.

Ni, M., Liang, X., Hou, L., Li, W., and He, C.: Submerged macrophytes regulate diurnal nitrous oxide emissions from a shallow eutrophic lake: A case study of Lake Wuliangsuhai in the temperate arid region of China. *Science of The Total Environment*, *811*, 152451. https://doi.org/10.1016/j.scitotenv.2021.152451, 2022a.

Ni, R., Xu, C., Shi, X., Yang, S., Li, L., Peng, X., and Song, L.: Acetoclastic methanogenesis pathway stability despite the high microbial taxonomic variability in the transition from acidogenesis to methanogenesis during food waste anaerobic digestion. *Journal of Cleaner Production*, *372*, 133758. https://doi.org/10.1016/j.jclepro.2022.133758, 2022b.

Ollivier, Q.R., Maher, D.T., Pitfield, C., and Macreadie, P.I.: Punching above their weight: large release of greenhouse gases from small agricultural dams. Glob. Chang. Biol. 25 (2), 721–732. https://doi.org/10.1111/gcb.14477, 2019.

Palacin-Lizarbe, C., Camarero, L., Hallin, S., Jones, C. M., and Catalan, J.: Denitrification rates in lake sediments of mountains affected by high atmospheric nitrogen deposition. Sci Rep 10, 3003. https://doi.org/10.1038/s41598-020-59759-w, 2020.

Peacock, M., Audet, J., Bastviken, D., Cook, S., Evans, C.D., Grinham, A., Holgerson, M. A., Högbom, L., Pickard, A.E., Zieliński, P., and Futter, M.N.: Small artificial waterbodies are widespread and persistent emitters of methane and carbon dioxide. Glob. Chang. Biol. 27 (20), 5109–5123. https://doi.org/10.1111/gcb.15762, 2021.

Peacock, M., Audet, J., Jordan, S., Smeds, J., and Wallin, M.B.: Greenhouse gas emissions from urban ponds are driven by nutrient status and hydrology. Ecosphere 10 (3), e02643. https://doi.org/10.1002/ecs2.2643, 2019.

Peretyatko, A., Symoens, J. J., and Triest, L.: Impact of macrophytes on phytoplankton in eutrophic peri-urban ponds, implications for pond management and restoration. *Belgian Journal of Botany*, 83-99. https://doi.org/10.2307/20794626 , 2007.

Raymond, P. A., Hartmann, J., Lauerwald, R., Sobek, S., McDonald, C., Hoover, M., Butman, D., Striegl, R., Mayorga, E., Humborg, C., Kortelainen, P., Dürr, H., Meybeck, M., Ciais, P., and Guth, P.: Global carbon dioxide emissions from inland waters. Nature, 503(7476), 355–359. https://doi.org/10.1038/nature12760, 2013.

Reis, P.C.J., Thottathil, S.D. and Prairie, Y.T. The role of methanotrophy in the microbial carbon metabolism of temperate lakes. *Nat Commun* 13, 43. https://doi.org/10.1038/s41467-021-27718-2, 2022.

Reitsema, R. E., Meire, P., and Schoelynck, J.: The future of freshwater macrophytes in a changing world: dissolved organic carbon quantity and quality and its interactions with macrophytes. *Frontiers in Plant Science*, *9*, 301954. https://doi.org/10.3389/fpls.2018.00629 , 2018.

Rocher-Ros, G., Stanley, E. H., Loken, L. C., Casson, N. J., Raymond, P. A., Liu, S., Amatulli, G., and Sponseller, R. A.: Global methane emissions from rivers and streams. Nature 621:530–535. https://doi.org/10.1038/s41586-023-06344-6, 2023.

Rosentreter, J. A., Borges, A. V., Deemer, B. R., Holgerson, M. A., Liu, S., Song, C., Melack, J., Raymond, P. A., Duarte, C. M., Allen, G. H., Olefeldt, D., Poulter, B., Battin, T. I., and Eyre, B. D.: Half of global methane emissions come from highly variable aquatic ecosystem sources. Nature Geoscience, 14(4), 225–230. https://doi.org/10.1038/s41561-021-00715-2, 2021.

Scandella, B. P., Varadharajan, C., Hemond, H. F., Ruppel, C., and Juanes, R.: A conduit dilation model of methane venting from lake sediments. Geophysical Research Letters, 38(6). https://doi.org/10.1029/2011GL046768, 2011.

Scheffer, M., Hosper, S. H., Meijer, M. L., Moss, B., and Jeppesen, E. (1993). Alternative equilibria in shallow lakes. *Trends in ecology & evolution*, *8*(8), 275-279. https://doi.org/10.1016/0169-5347(93)90254-M

Schulz S., Matsuyama, H., and Conrad, R.: Temperature dependence of methane production from different precursors in a profundal sediment (Lake Constance) FEMS Microbiology Ecology, 22, 207-213; https://doi.org/10.1111/j.1574-6941.1997.tb00372.x, 1997.

Schulz S., and Conrad, R.: Influence of temperature on pathways to methane production in the permanently cold profundal sediment of Lake Constance. FEMS Microbiology Ecology 20 l- I4; https://doi.org/10.1111/j.1574-6941.1996.tb00299.x, 1996.

Singh, S.N., Kulshreshtha, K., and Agnihotri, S.: Seasonal dynamics of methane emission from wetlands. Chemosphere Glob. Chang. Sci. 2 (1), 39–46. https://doi.org/10.1016/S1465-9972(99)00046-X, 2000.

https://doi.org/10.5194/egusphere-2024-1315
Preprint. Discussion started: 14 May 2024

Stanley, E. H., Casson, N. J., Christel, S. T., Crawford, J. T., Loken, L. C., and Oliver, S. K.: The ecology of methane in streams and rivers: patterns, controls, and global significance. Ecological Monographs, 86(2), 146–171. https://doi.org/10.1890/15-1027, 2016.

Taoka, T., Iwata, H., Hirata, R., Takahashi, Y., Miyabara, Y., and Itoh, M.: Environmental controls of diffusive and ebullitive methane emissions at a subdaily time scale in the littoral zone of a midlatitude shallow lake. Journal of Geophysical Research: Biogeosciences, 125, e2020JG005753. https://doi.org/10.1029/2020JG005753, 2020.

Theus, M. E., Ray, N. E., Bansal, S., and Holgerson, M. A.: Submersed macrophyte density regulates aquatic greenhouse gas emissions. *Journal of Geophysical Research: Biogeosciences*, *128*(10), https://doi.org/10.1029/2023JG007758, 2023.

Tokida, T., Miyazaki, T., Mizoguchi, M., Nagata, O., Takakai, F., Kagemoto, A., and Hatano, R.: Falling atmospheric pressure as a trigger for methane ebullition from peatland. Global Biogeochemical Cycles, 21(2). https://doi.org/10.1029/2006GB002790, 2007.

van Bergen, T.J.H.M., Barros, N., Mendonça, R., Aben, R.C.H., Althuizen, I.H.J., Huszar, V., Lamers, L.P.M., Lürling, M., Roland, F., and Kosten, S.: Seasonal and diel variation in greenhouse gas emissions from an urban pond and its major drivers. Limnol. Oceanogr. 64 (5), 2129–2139. https://doi.org/10.1002/lno.11173, 2019.

Varadharajan, C., and Hemond, H. F.: Time-series analysis of high-resolution ebullition fluxes from a stratified, freshwater lake. Journal of Geophysical Research: Biogeosciences, 117(G2). https://doi.org/10.1029/2011JG001866, 2012.

Verpoorter, C., Kutser, T., Seekell, D. A., and Tranvik, L. J.: A global inventory of lakes based on high-resolution satellite imagery. *Geophysical Research Letters*, *41*(18), 6396-6402. https://doi.org/10.1002/2014GL060641, 2014.

Wang, T., Zhumabieke, M., Zhang, N., Liu, C., Zhong, J., Liao, Q., and Zhang, L.: Variable promotion of algae and macrophyte organic matter on methanogenesis in anaerobic lake sediment. *Environmental Research*, *237*, 116922. https://doi.org/10.1016/j.envres.2023.116922, 2023.

Wang, Z., Wang, S., Hu, Y., Du, B., Meng, J., Wu, G., Liu, H., and Zhan, X.: Distinguishing responses of acetoclastic and hydrogenotrophic methanogens to ammonia stress in mesophilic mixed cultures. *Water Research*, *224*, 119029. https://doi.org/10.1016/j.watres.2022.119029, 2022.

Wanninkhof, R.: Relationship between gas exchange and wind speed over the ocean. J. Geophys. Res. 97, 7373–7381. https://doi.org/10.1029/92JC00188, 1992.

Webb, J.R., Leavitt, P.R., Simpson, G.L., Baulch, H.M., Haig, H.A., Hodder, K.R., and Finlay, K.: Regulation of carbon dioxide and methane in small agricultural reservoirs: optimizing potential for greenhouse gas uptake. Biogeosciences 16 (21), 4211–4227. https://doi.org/10.5194/bg-16-4211-2019, 2019.

Weiss, R. F.: Determinations of carbon dioxide and methane by dual catalyst flame ionization chromatography and nitrous oxide by electron capture chromatography. J. Chromatogr. Sci. 19, 611–616. https://doi.org/10.1093/chromsci/19.12.611, 1981.

West, W. E., Coloso, J. J., and Jones, S. E.: Effects of algal and terrestrial carbon on methane production rates and methanogen community structure in a temperate lake sediment. Freshw. Biol. 57, 949–955. https://doi.org/10.1111/j.1365-2427.2012.02755.x, 2012.

Whiticar, M. J., Faber, E., and Schoell, M.: Biogenic methane formation in marine and freshwater environments: CO2 reduction vs. acetate fermentation—isotope evidence. *Geochimica et Cosmochimica Acta*, *50*(5), 693-709.https://doi.org/10.1016/0016-7037(86)90346-7, 1986.

Wik, M., Crill, P. M., Varner, R. K., and Bastviken, D.: Multiyear measurements of ebullitive methane flux from three subarctic lakes. J. Geophys. Res. Biogeosciences 118:791 1307–1321. https://doi.org/10.1002/jgrg.20103, 2013.

Wik, M., Thornton, B. F., Bastviken, D., MacIntyre, S., Varner, R. K., and Crill, P. M.: Energy input is primary controller of methane bubbling in subarctic lakes. *Geophysical Research Letters*, *41*(2), 555-560. https://doi.org/10.1002/2013GL058510, 2014.

Xun, F., Feng, M., Ma, S., Chen, H., Zhang, W., Mao, Z., Zhou, Y., Xiao, Q, Wu, Q. L., and Xing, P.: Methane ebullition fluxes and temperature sensitivity in a shallow lake. *Science of The Total Environment*, *912*, 169589. https://doi.org/10.1016/j.scitotenv.2023.169589, 2024.

Yan, X., Xu, X., Ji, M., Zhang, Z., Wang, M., Wu, S., Wang, G., Zhang, C., and Liu, H.: Cyanobacteria blooms: A neglected facilitator of CH4 production in eutrophic lakes. *Science of the total environment*, *651*, 466-474. https://doi.org/10.1016/j.scitotenv.2018.09.197, 2019.

Yang, Z., Zhao, Y., and Xia, X.: Nitrous oxide emissions from Phragmites australis-dominated zones in a shallow lake. *Environmental pollution*, *166*, 116-124. https://doi.org/10.1016/j.envpol.2012.03.006, 2012.

Yentsch, C.S., and Menzel, D.W.: A method for the determination of phytoplankton chlorophyll and phaeophytin by fluorescence. In: Deep Sea Research and Oceanographic Abstracts, 10. Elsevier, pp. 221–231. https://doi.org/10.1016/0011-7471(63)90358-9, 1963.

https://doi.org/10.5194/egusphere-2024-1315
Preprint. Discussion started: 14 May 2024

Zhao, K., Tedford, E. W., Zare, M., and Lawrence, G. A.: Impact of atmospheric pressure variations on methane ebullition and lake turbidity during ice-cover. Limnology and Oceanography Letters, 6(5), 253-261. https://doi.org/10.1002/lol2.10201, 2021.